Supporting Information

Cu(I)-Based Metal–Organic Framework-Derived Core-Shell Composites for Carbon Dioxide Conversion to Oxazolidinones

Xiaoci Zhang,[a, b] Ce Liu,[a] Yanxin Liu,[a, b] Rongrong Fan,[a, b] Feng Shi*[a] and Xinjiang Cui*[a]

[a] State Key Laboratory of Low Carbon Catalysis and Carbon Dioxide Utilization, State Key Laboratory for Oxo Synthesis and Selective Oxidation, Lanzhou Institute of Chemical Physics, Chinese Academy of Sciences, No.18, Tianshui Middle Road, Lanzhou 730000, People's Republic of China.

[b] University of Chinese Academy of Sciences, No. 19A, Yuquanlu, Beijing 100049, People's Republic of China.

* E-mail: xinjiangcui@licp.cas.cn.

Contents

1. Experimental Section

1.1 Materials

The copper(II) chloride dihydrate ($CuCl_2 \cdot 2H_2O$), zinc nitrate hexahydrate ($Zn(NO_3)_2 \cdot 6H_2O$), cobaltous nitrate hexahydrate ($Co(NO_3)_2 \cdot 6H_2O$), sodium hydroxide, sodium dodecyl benzene sulfonate (SDBS), L-ascorbic acid, polyvinyl pyrrolidone (PVP), 2-methylimidazole, ethanol, acetonitrile, dichloroethane, N,N-dimethylformamide, dimethyl sulfoxide, tetrahydrofuran, ethyl acetate, methanol, toluene, 2-methyl-3-butyn-2-ol, n-butylamine, and other chemicals were purchased from Energy Chemical, Innochem, TCI, Aladdin and Macklin. High purity gases, including CO_2 (> 99.9%), argon gas (> 99.99%), were supplied by a gas supplier. All reagents were commercially available and used without further purification, unless stated otherwise.

1.2 Catalyst preparation

Synthesis of Cu_2O and CuO.

Rhombic dodecahedral Cu_2O nanoparticles were synthesized according to the literature with a slight modification.[1] Initially, $CuCl_2 \cdot 2H_2O$ (8.0 mmol) was weighted and dissolved in 80.0 mL deionized water. Separately, SDBS (16.0 mmol), sodium hydroxide (80.0 mmol), and L-ascorbic acid (16.0 mmol) were individually weighed and dissolved in 20.0 mL and 40.0 mL deionized water, respectively. The prepared SDBS solution was added and stirred for 10 minutes at room temperature. Subsequently, the sodium hydroxide solution was gradually added, causing the solution to turn light blue. The L-ascorbic acid solution was then rapidly added, and the mixture was stirred continuously for 2 hours. Finally, the resulting yellow precipitate was collected via centrifugation and washed with a water/ethanol mixture (1:1, v/v) until neutral. The synthesized sample was dried in a vacuum oven at 60 °C for 12 hours. To obtain CuO, the Cu_2O was further pyrolyzed at 400 °C for 2 hours in a muffle furnace, with a heating rate of 5 °C min^{-1}.

Synthesis of ZIF-8.

Typically, $Zn(NO_3)_2 \cdot 6H_2O$ (20.0 mmol) and 2-methylimidazole (80.0 mmol) were dissolved in 80.0 mL methanol, respectively.[2] The 2-methylimidazole solution was then rapidly combined with the zinc nitrate solution, followed by continuous stirring at room temperature for 6 hours. The resulting white precipitate was collected by centrifugation, washed multiple times with methanol, and dried under vacuum at 60 °C for 12 hours.

Synthesis of Cu_2O@ZIF-8 and CuO@ZIF-8.

Cu_2O@ZIF-8 was synthesized using a surfactant-assisted encapsulation method. Initially, Cu_2O (500.0 mg) and PVP (2.0 g) were dissolved in 20.0 mL methanol, while $Zn(NO_3)_2 \cdot 6H_2O$ (5.05 mmol) and PVP (0.5 g) were dissolved in a separate 20.0 mL methanol. Additionally, 2-

methylimidazole (7.32 mmol) and PVP (0.5 g) were dissolved in 40.0 mL methanol. The zinc nitrate and 2-methylimidazole solutions were sequentially added to the Cu_2O solution, followed by stirring at room temperature for 4 hours. The resulting powder was collected via centrifugation, washed extensively with methanol, and dried in a vacuum oven at 60 °C for 6 hours. In addition, CuO@ZIF-8 composites were synthesized by substituting CuO for Cu_2O in the process.

1.3 Catalyst characterization

The morphology and elements distribution were analyzed using high-angle annular dark-field scanning transmission electron microscopy (HAADF–STEM, FEI-Titan Cubed Themis G2 300) with energy dispersive spectroscopy (EDS). X-ray diffraction (XRD) was performed on a Smartlab-SE diffractometer with Cu Kα (1.5406 Å) radiation. The XRD patterns are scanned in the 2θ range of 10–80°. For the data interpretation, the software WinXpow (STOE) and the database of Powder Diffraction File (PDF) of the International Centre of Diffraction Data (ICDD) were used. X-ray photoelectron spectroscopy (XPS) and Auger electron spectroscopy (AES) were performed using a Thermo Fisher Scientific photoemission spectrometer equipped with a monochromatic Al Kα (1486.6 eV) source and a step size of 0.1 eV. The samples were fixed to a stainless steel sample holder by using double-sided adhesive carbon tape. The electron binding energies of each spectrum were calibrated against a standard C 1s contamination peak at 284.8 eV to correct for charging effects, and the peaks were fitted by the Avantge program. Fourier transform infrared (FT-IR) spectrum were recorded with a Bruker VERTEX 70FTIR spectrometer.

The specific surface area, micropore volume, and pore size distribution were determined by Barrett, Joyner, and Halenda (BJH) measurements via nitrogen adsorption-desorption isotherms at 77 K (Autosorb iQ2, Quantachrome). Thermogravimetric analysis (TGA) was performed using the METTLER TOLEDO simultaneous thermal analyzer, with samples dried at 60 °C for 6 hours prior to analysis. The samples were then heated to 800 °C under nitrogen flow at 10 °C min^{-1} to generate TGA curves. Additionally, ^{1}H and ^{13}C liquid nuclear magnetic resonance (NMR) spectra were recorded on the Bruker Avance III HD 400 MHz NMR spectrometer with deuterated chloroform ($CDCl_3$), unless otherwise noted.

1.4 The three-component coupling cyclization of CO_2, propargyl alcohols and amines

In a standard procedure, propargyl alcohol (1.0 mmol), n-butylamine (1.5 mmol), catalyst (50 mg), and acetonitrile (2.0 mL) were combined in a 100 mL stainless steel autoclave. The reactor was purged with carbon dioxide several times before being pressurized to 2.0 MPa at room temperature. The reaction mixture was stirred at 100 °C for 24 hours. After completion, the reaction was quenched using an ice-water bath to slowly release carbon dioxide. The catalyst was then washed with fresh MeOH (3 × 10 mL) and dried under vacuum at 60 °C for 6 hours in preparation

for the next cycle. The yield was determined by gas chromatography, using 1,3,5-trimethylbenzene (0.5 mmol) as an internal standard. The product was purified by column chromatography (silica gel, petroleum ether: ethyl acetate, 20:1–2:1) and characterized by ^{1}H and ^{13}C NMR spectroscopy.

1.5 Hot filtration test

In a standard procedure, propargyl alcohol (1.0 mmol), n-butylamine (1.5 mmol), catalyst (50 mg), and acetonitrile (2.0 mL) were combined in a 100 mL stainless steel autoclave. The reactor was purged with carbon dioxide several times before being pressurized to 2.0 MPa at room temperature. The reaction mixture was then stirred at 100 °C for 6 hours. After completion, the reaction was quenched using an ice-water bath to slowly release carbon dioxide. The residue was centrifuged, and determined the yield by gas chromatography. Subsequently, the reaction solution was returned to the reactor, and the process were repeated, with the yield being monitored at various intervals by gas chromatography.

1.6 Products analysis

Qualitative analysis was conducted using Gas Chromatography-Mass Spectrometry (GC-MS) (Agilent 5977A MSD), while quantitative analysis was performed via Gas Chromatography (GC) (Agilent 7890). The conversion rate of the reactant and the product yield were determined using an external standard method. The initial temperature was set at 50 °C for 1 minute, followed by a heating rate of 10 °C min^{-1} until it reached 60 °C. The temperature was then maintained at 60 °C for 1 minute before being increased to 280 °C at a rate of 20 °C min^{-1}. Finally, the temperature was held at 280 °C for 2 minutes.

The corresponding formulas for calculating conversion and yield were defined as follows:

$$\text{Substrate Conversion} = \frac{\text{molar of substrate converted}}{\text{molar of substrate fed}} \times 100\%$$

$$\text{Product Yield} = \frac{\text{molar of product produced}}{\text{molar of substrate fed}} \times 100\%$$

2. Supplementary Figures

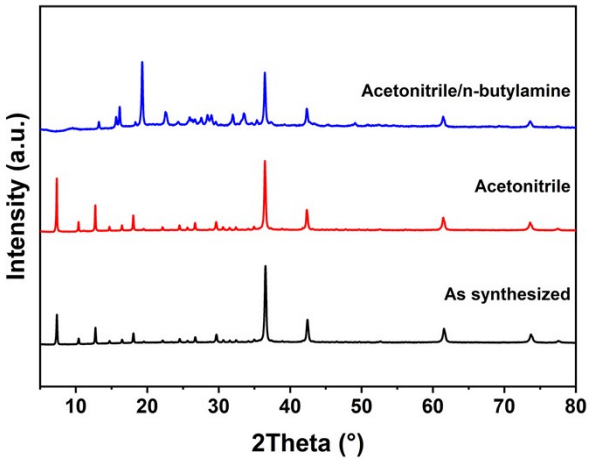

Fig. S1 The XRD patterns of Cu_2O@ZIF-8 in different condition treatments: immersed in acetonitrile, acetonitrile and n-butylamine under CO_2 for 24 h, respectively.

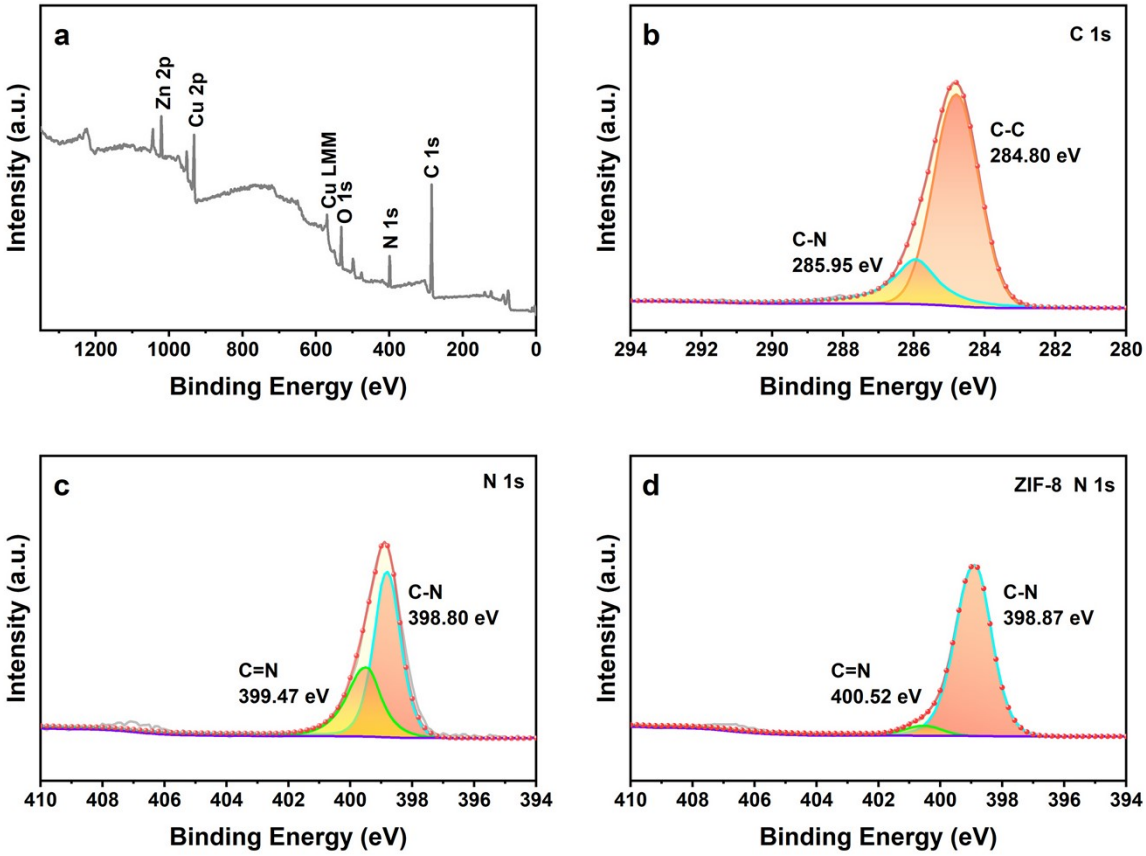

Fig. S2 High resolution XPS spectrums of Cu_2O@ZIF-8: (a) XPS survey spectra, (b) C 1s spectra and (c) N 1s spectra. (d) N 1s spectra of ZIF-8.

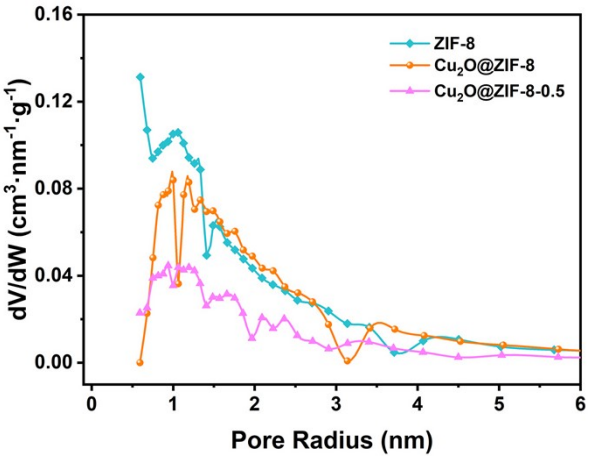

Fig. S3 The pore size distribution of ZIF-8, Cu_2O@ZIF-8-0.5 and Cu_2O@ZIF-8.

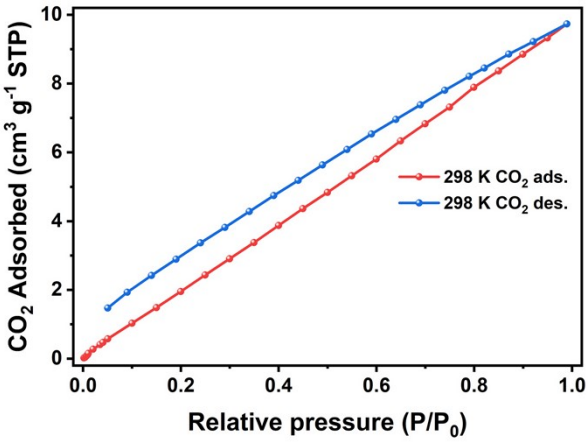

Fig. S4 CO_2 adsorption-desorption isotherms of Cu_2O@ZIF-8 at 298 K.

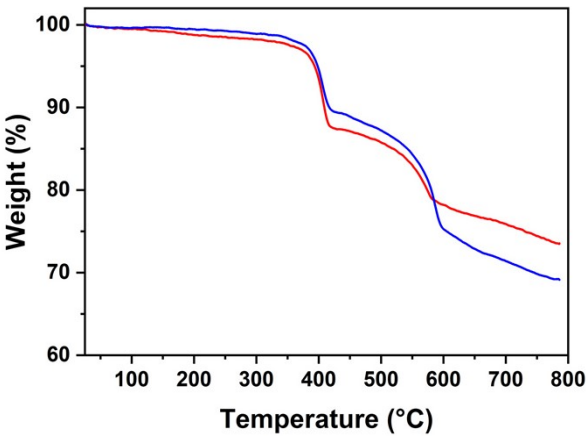

Fig. S5 The TGA weight decomposition curves of Cu_2O@ZIF-8 (red line) and Cu_2O@ZIF-8-2 (blue line).

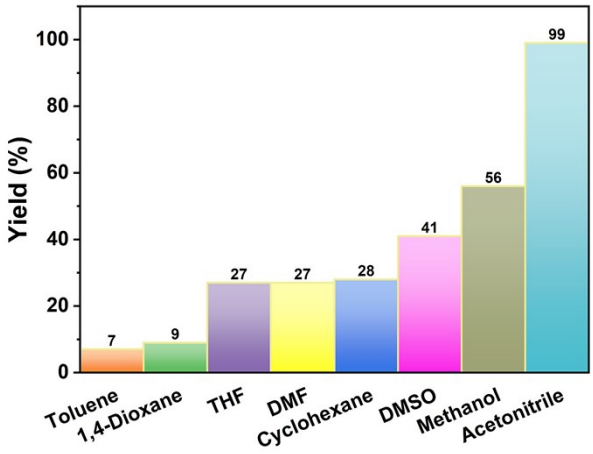

Fig. S6 The effect of different solvents on three-component coupling cyclization reaction.

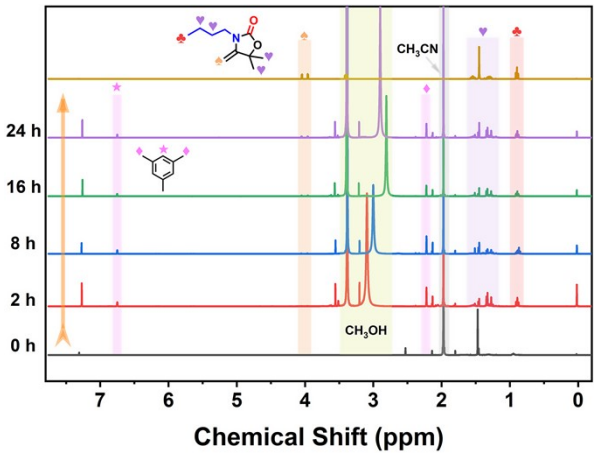

Fig. S7 ^{1}H NMR spectra of the three-component coupling reaction of 2-methyl-3-butyn-2-ol at various reaction intervals (0, 2, 8, 16 and 24 h), with methanol used during the dilution process.

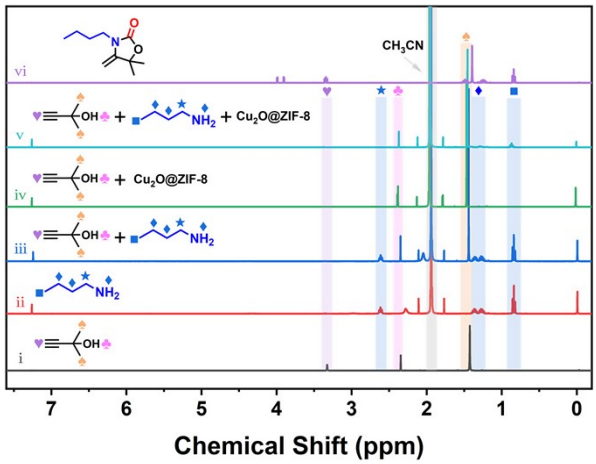

Fig. S8 ^{1}H NMR spectra for mechanism investigation of the interaction of Cu_2O@ZIF-8 with n-butylamine and 2-methyl-3-butyn-2-ol.

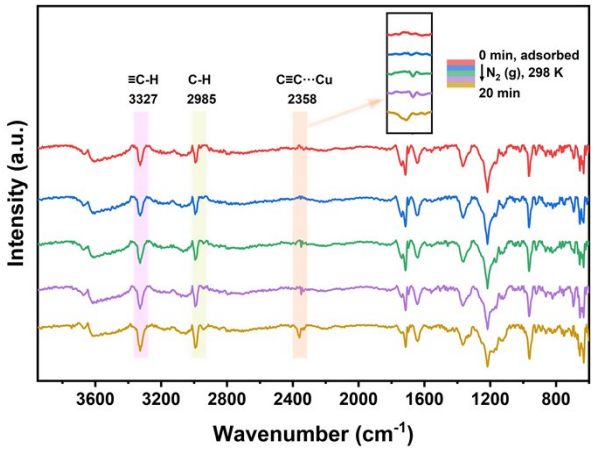

Fig. S9 In situ FT-IR spectra of 2-methyl-3-butyn-2-ol and activated by Cu_2O@ZIF-8.

During the experiment, 2-methyl-3-butyn-2-ol was saturated adsorbed on the surface of the catalyst using N_2 bubbling, followed by purging with N_2, and the infrared spectra revealed a gradual emerging absorption peak near 2358 cm^{-1}. This peak located in the stretching vibration region of the unsaturated triple bond and the cumulative double bond. Given that the system lacked CO_2, whose asymmetric stretching vibration appeared around 2345 cm^{-1}, the observed peak could be attributed to the formation of a C≡C···Cu bond, indicating an interaction between Cu and the C≡C bond. This likely arose from Cu(I) induced polarization of the C≡C bond, which altered the electronic environment and consequently caused a blueshift in the C≡C stretching vibrational peak from approximately 2200 cm^{-1} to higher wavenumber.[3,4]

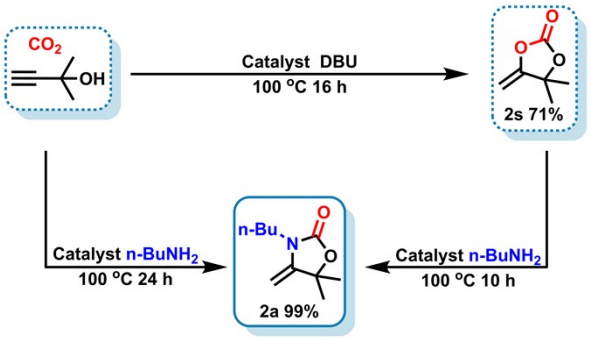

Fig. S10 Control experiments for the three-component coupling cyclization reaction.

3. Supplementary Tables

Table S1. The three-component coupling formation of oxazolidinones by 2-methyl-3-butyn-2-ol.[a]

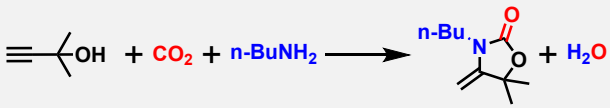

Entry	Catalysts	T [°C]	P [MPa]	T [h]	Yield [%]
1[b]	Cu_2O@ZIF-8	100	2	24	65
2[c]	Cu_2O@ZIF-8	100	2	24	85
3[d]	Cu_2O@ZIF-8	100	2	24	80
4	Cu_2O and ZIF-8	100	2	24	36
5	Cu_2O@ZIF-8-Ar	100	2	24	33
6	CuO@ZIF-8	100	2	24	38
7	CuO	100	2	24	21

[a] Reaction conditions: 2-methyl-3-butyn-2-ol (1.0 mmol), n-butylamine (1.5 mmol), 50.0 mg catalyst, CH_3CN (2.0 mL), 2.0 MPa CO_2, 100 °C and 24 h. The yield was determined by GC analysis using mesitylene (0.5 mmol) as the internal standard. [b] 20.0 mg catalyst. [c] 40.0 mg catalyst. [d] 100.0 mg catalyst.

Table S2. Relative contents of the catalysts.

Catalyst	Cu(wt%)	Zn(wt%)
Cu_2O@ZIF-8	67.96	12.93
Cu_2O@ZIF-8-2	69.55	23.77

Actual content of Cu and Zn determined by ICP-OES.

Table S3. Catalytic performance comparison of various catalysts for the three-component coupling cyclization.

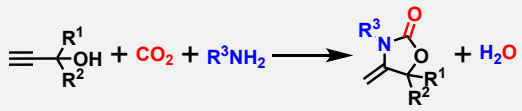

Catalyst[a]	Reaction conditions	Yield [%]	TON	Ref.
Cu_2O@ZIF-8	2-methyl-3-butyn-2-ol (1 mmol), n-$BuNH_2$ (1.5 mmol) Solvent (2 mL CH_3CN), CO_2 (2 MPa), 100 °C for 24 h	99	21.3	This work
9.8%-Cu/Co_3O_4	2-methyl-3-butyn-2-ol (5 mmol), n-$BuNH_2$ (7.5 mmol) Solvent free, CO_2 (3 MPa), 120 °C for 24 h	99	10.8	5
MOF-SO_3Ag/DBU	2-methyl-3-butyn-2-ol (2 mmol), n-$BuNH_2$ (2 mmol) Solvent (2 mL DMF), CO_2 (0.1 MPa), RT for 26 h	99	66.0	6
CNT-NHC-Cu	2-methyl-3-butyn-2-ol (10 mmol), n-$BuNH_2$ (20 mmol) Solvent free, CO_2 (5 MPa), 120 °C for 24 h	90	51.4	7
TMOF-3-Ag/PPh_3	2-methyl-3-butyn-2-ol (0.2 mmol), n-$BuNH_2$ (0.2 mmol) Solvent (2 mL DMSO), CO_2 (0.1 MPa), 50 °C for 12 h	99	2.0	8
Ag@TFPNDA-COF	2-methyl-3-butyn-2-ol (2 mmol), Benzylamine (2 mmol) Solvent free, CO_2 (0.1 MPa), RT for 4 h	92	117.5	9
Ag_2WO_4/PPh_3	2-methyl-3-butyn-2-ol (5 mmol), n-$BuNH_2$ (5 mmol) Solvent free, CO_2 (0.5 MPa), 40 °C for 12 h	95	475.0	10
AgOAc	2-methyl-3-butyn-2-ol (2 mmol), n-$BuNH_2$ (2 mmol) Solvent free, CO_2 (8 MPa), 120 °C for 24 h	98	19.6	11
CuCl	2-methyl-3-butyn-2-ol (2 mmol), n-$BuNH_2$ (4 mmol) Solvent free, CO_2 (0.1 MPa), 60 °C for 24 h	81	16.2	12
CuI	2-methyl-3-butyn-2-ol (2 mmol), n-$BuNH_2$ (2 mmol) Solvent free, CO_2 (12 MPa), 80 °C for 24 h	89	17.8	13
CuI/$[P_{4444}][Im]$	2-methyl-3-butyn-2-ol (1 mmol), n-$BuNH_2$ (1 mmol) Solvent free, CO_2 (0.1 MPa), 30 °C for 24 h	87	8.7	14
$[DMIm][BF_4]$	2-methyl-3-butyn-2-ol (10 mmol), n-$BuNH_2$ (10 mmol) Solvent (3 mL ILs), CO_2 (5 MPa), 120 °C for 10 h	84	820.2	15
CuCl/$[BMIm][BF_4]$	1-ethynylcyclohexan-1-ol (10 mmol), n-$BuNH_2$ (10 mmol) Solvent (3 mL ILs), CO_2 (2.5 MPa), 100 °C for 10 h	80	40.0	16
MTBD	2-methyl-3-butyn-2-ol (5 mmol), n-$BuNH_2$ (5 mmol) Solvent free, CO_2 (liquid 44 g), RT for 24 h	78	7.8	17
2,2',2"-terpyridine	2-methyl-3-butyn-2-ol (2 mmol), Benzylamine (4 mmol) Solvent free, CO_2 (3 MPa), 140 °C for 15 h	85	34.0	18

DBU: 1,8-Diazabicyclo[5.4.0]undec-7-ene

$[DMIm][BF_4]$: 1-Decyl-3-methylimidazolium tetrafluoroborate

$[BMIM][BF_4]$: 1-Butyl-3-methylimidazolium tetrafluoroborate

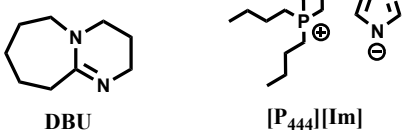

DBU **$[P_{444}][Im]$** **MTBD**

[a] The abbreviations and chemical structures of the catalysts listed in Table S3.

4. NMR Spectra

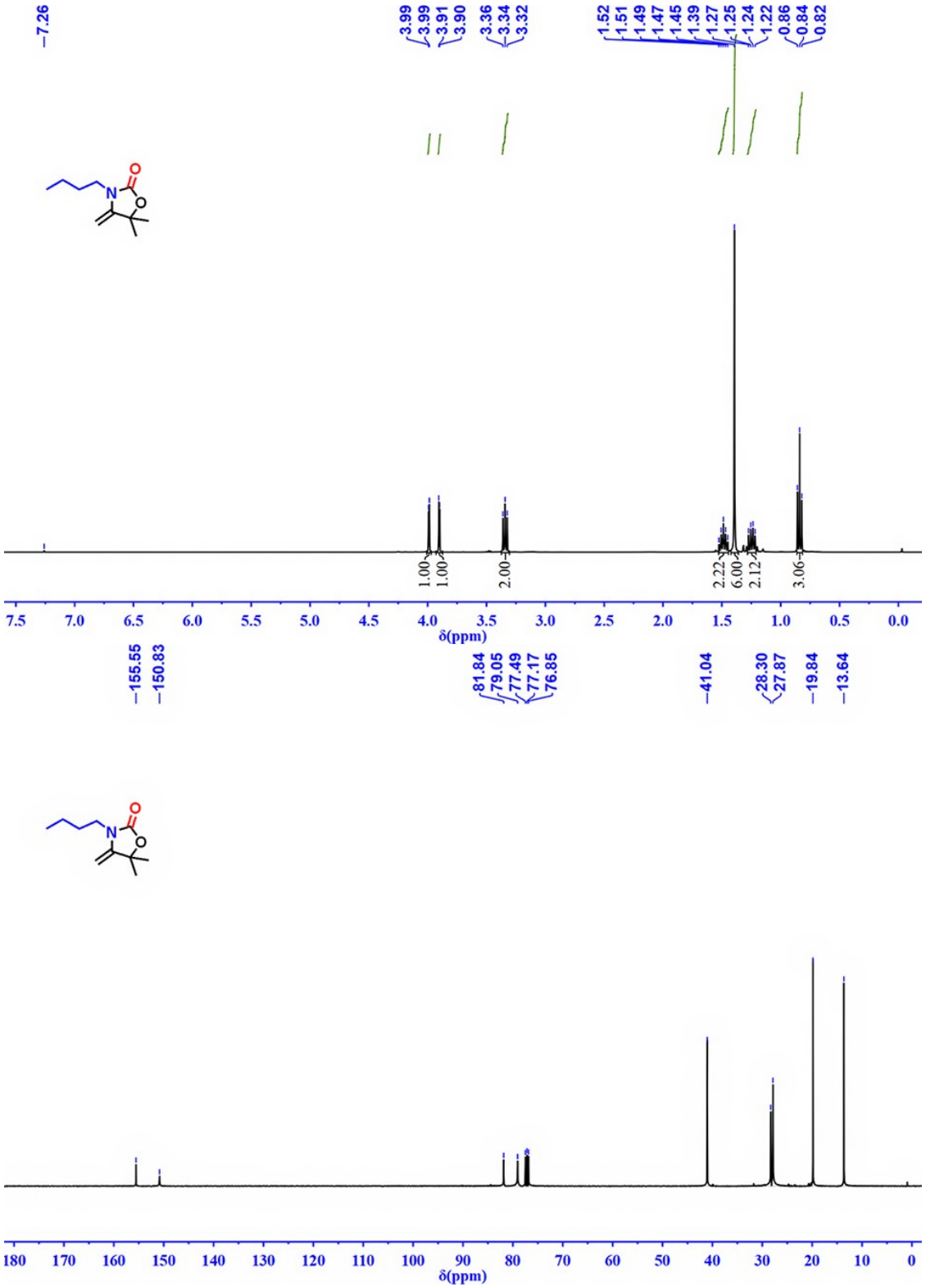

Fig. S11 ^{1}H and ^{13}C NMR of 3-butyl-5,5-dimethyl-4-methyleneoxazolidin-2-one (**2a**). ^{1}H NMR (400 MHz, Chloroform-d): δ 4.00 – 3.98 (d, J=2.9, 1H), 3.91 – 3.89 (d, J=2.9, 1H), 3.37 – 3.32 (m, 2H), 1.53 – 1.45 (p, J=7.5, 2H), 1.40 – 1.38 (s, 6H), 1.28 – 1.21 (dd, J=7.5, 15.1, 2H), 0.86 – 0.82 (t, J=7.4, 3H). ^{13}C NMR (101 MHz, $CDCl_3$): δ 155.55, 150.83, 81.84, 79.05, 41.04, 28.30, 27.87, 19.84, 13.64.

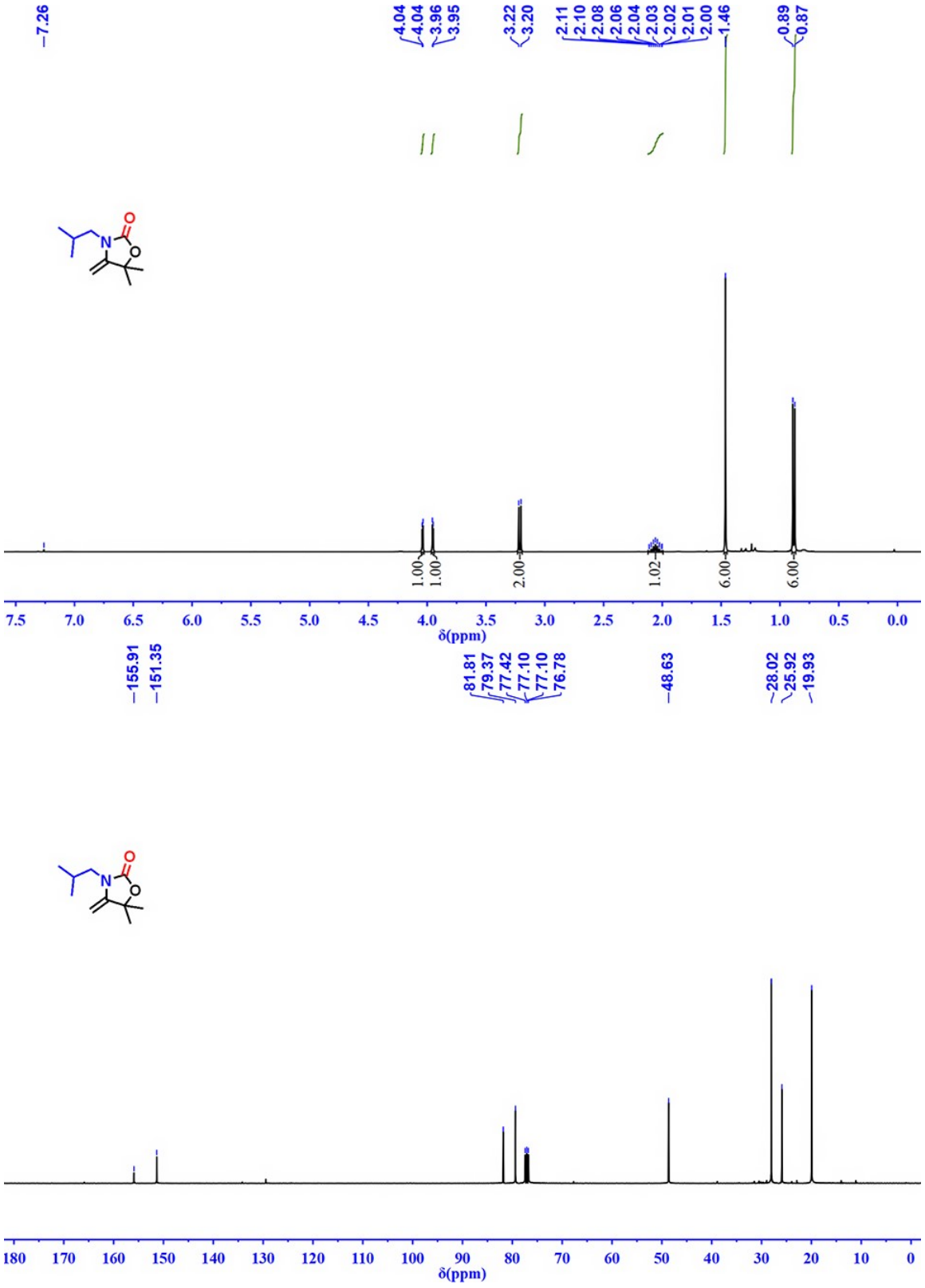

Fig. S12 ^{1}H and ^{13}C NMR of 3-isobutyl-5,5-dimethyl-4-methyleneoxazolidin-2-one (**2b**). ^{1}H NMR (400 MHz, Chloroform-d): δ 4.05 – 4.03 (d, J=2.9, 1H), 3.97 – 3.94 (d, J=2.9, 1H), 3.23 – 3.19 (d, J=7.6, 2H), 2.12 – 1.99 (m, 1H), 1.48 – 1.45 (s, 6H), 0.90 – 0.87 (d, J=6.7, 6H). ^{13}C NMR (101 MHz, $CDCl_3$): δ 155.91, 151.35, 81.81, 79.37, 48.63, 28.02, 25.92, 19.93.

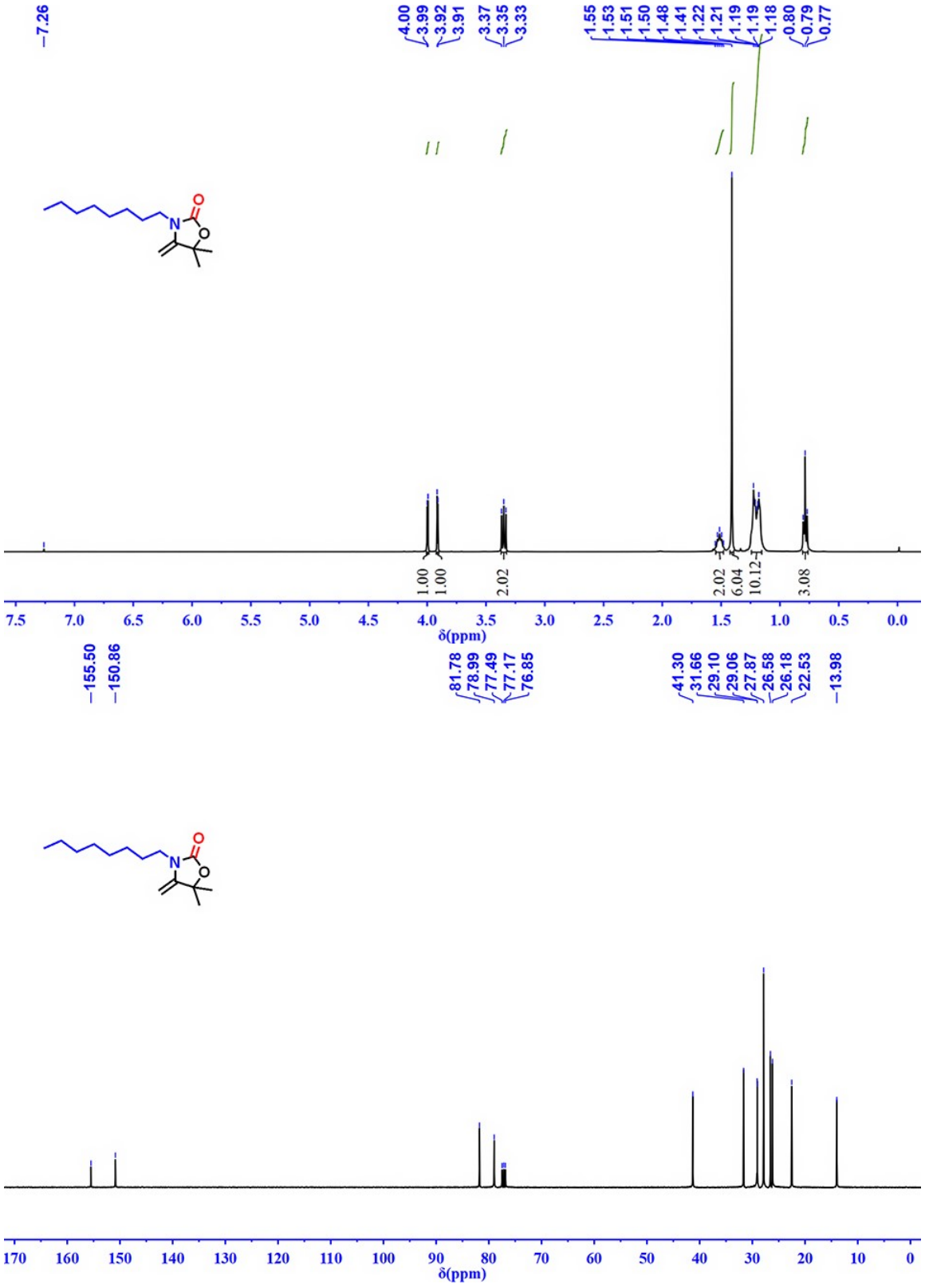

Fig. S13 ^{1}H and ^{13}C NMR of 5,5-dimethyl-4-methylene-3-octyloxazolidin-2-one (**2c**). ^{1}H NMR (400 MHz, Chloroform-d): δ 4.01 – 3.99 (d, J=2.9, 1H), 3.92 – 3.90 (d, J=2.9, 1H), 3.37 – 3.32 (m, 2H), 1.55 – 1.48 (m, 2H), 1.42 – 1.39 (s, 6H), 1.24 – 1.15 (m, 10H), 0.81 – 0.76 (m, 3H). ^{13}C NMR (101 MHz, $CDCl_3$): δ 155.50, 150.86, 81.78, 78.99, 41.30, 31.66, 29.10, 29.06, 27.87, 26.58, 26.18, 22.53, 13.98.

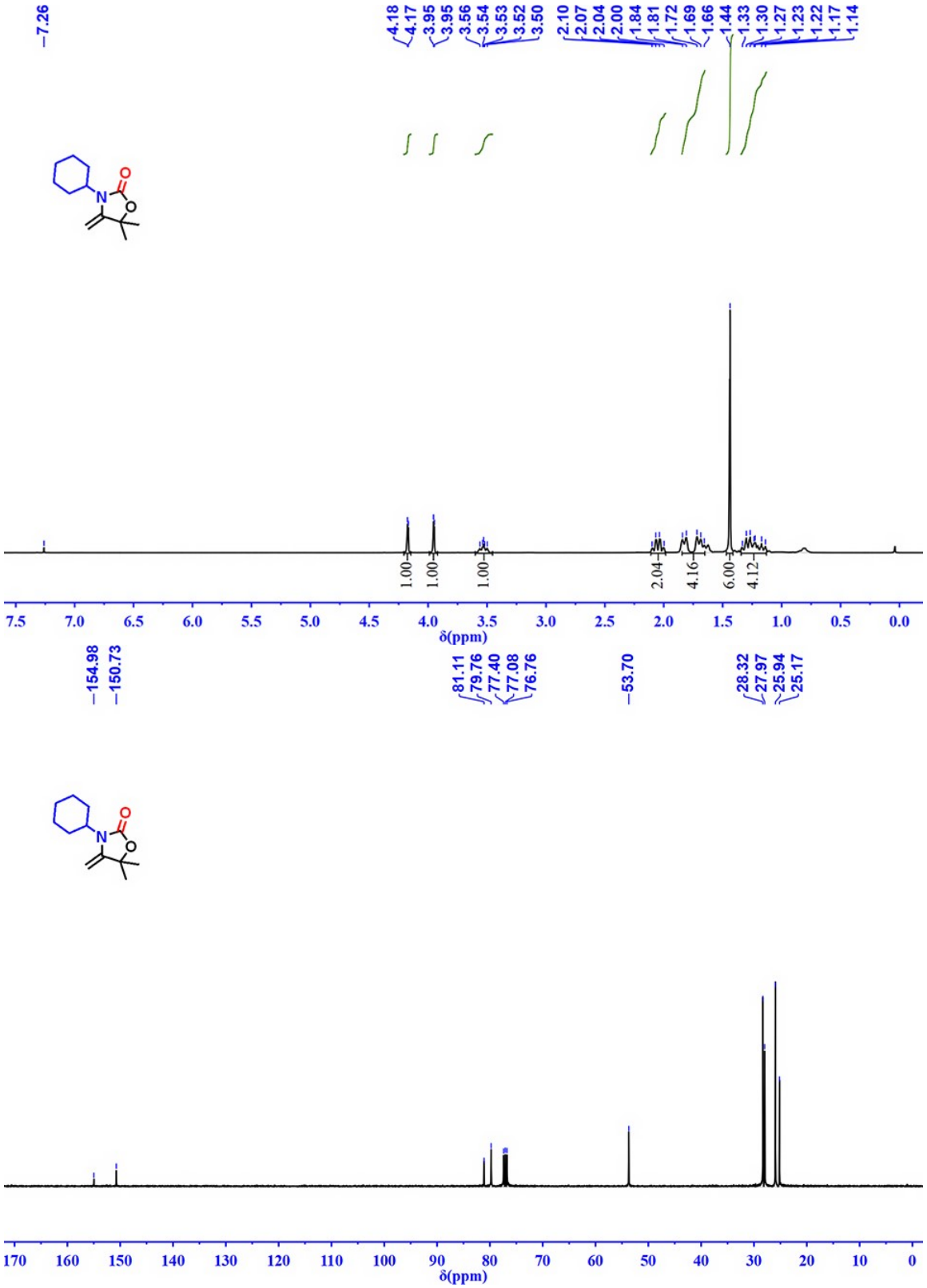

Fig. S14 ^{1}H and ^{13}C NMR of 3-cyclohexyl-5,5-dimethyl-4-methyleneoxazolidin-2-one (**2d**). ^{1}H NMR (400 MHz, Chloroform-d): δ 4.21 – 4.15 (d, J=2.9, 1H), 3.99 – 3.92 (d, J=3.0, 1H), 3.60 – 3.45 (m, 1H), 2.11 – 1.98 (q, J=14.1, 15.8, 2H), 1.85 – 1.65 (m, 4H), 1.47 – 1.41 (s, 6H), 1.34 – 1.13 (m, 4H). ^{13}C NMR (101 MHz, $CDCl_3$): δ 154.98, 150.73, 81.11, 79.76, 53.70, 28.32, 27.97, 25.94, 25.17.

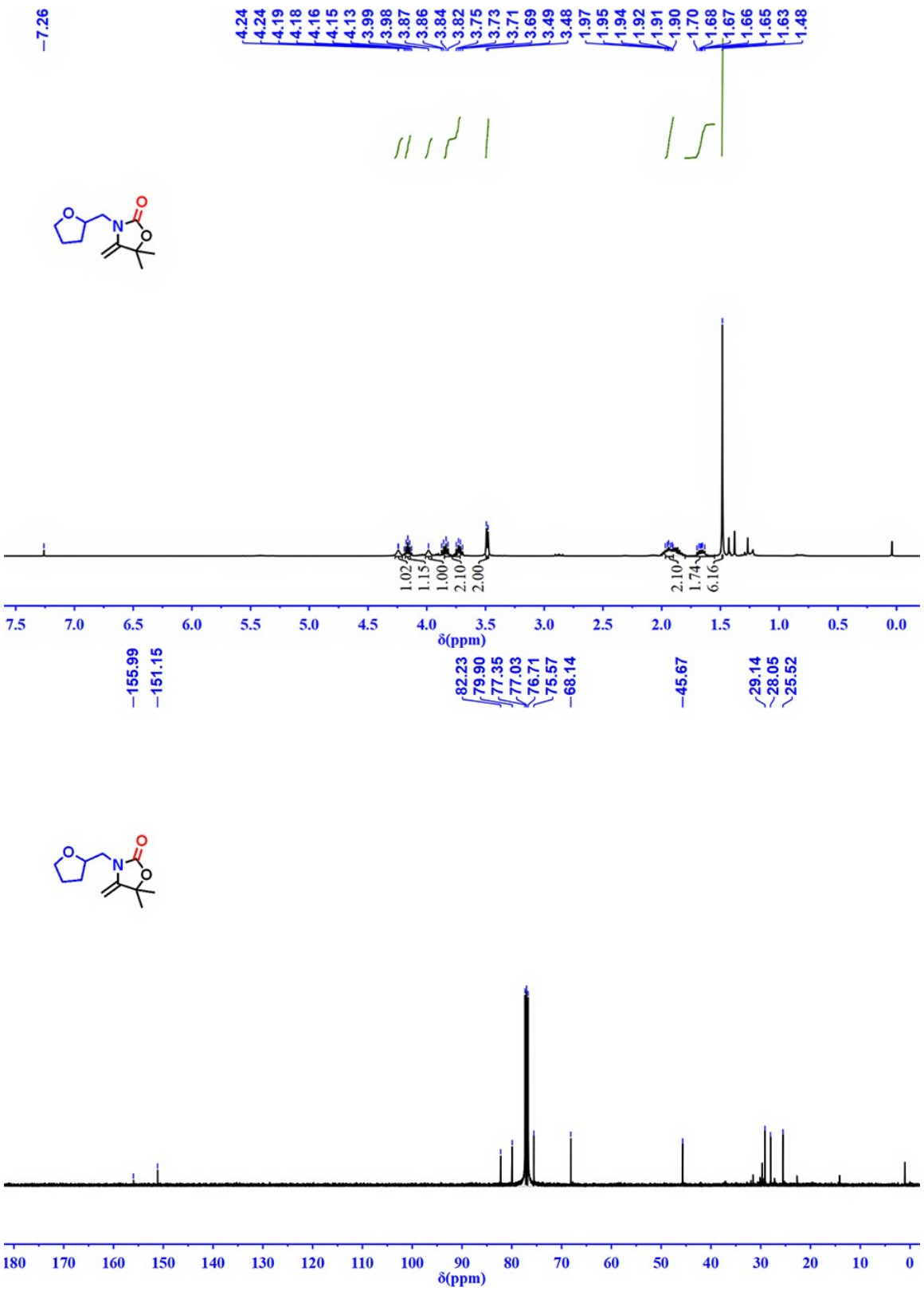

Fig. S15 ^{1}H and ^{13}C NMR of 5,5-dimethyl-4-methylene-3-((tetrahydrofuran-2-yl)methyl)oxazolidin-2-one (**2e**). ^{1}H NMR (400 MHz, Chloroform-d): δ 4.27 – 4.21 (m, 1H), 4.18 – 4.14 (m, 1H), 4.01 – 3.96 (m, 1H), 3.85 – 3.72 (m, 2H), 3.50 – 3.47 (d, J=5.7, 2H), 1.97 – 1.90 (m, 2H), 1.80 – 1.55 (m, 2H), 1.49 – 1.48 (s, 6H). ^{13}C NMR (101 MHz, $CDCl_3$): δ 155.99, 151.15, 82.23, 79.90, 75.57, 68.14, 45.67, 29.14, 28.05, 25.52.

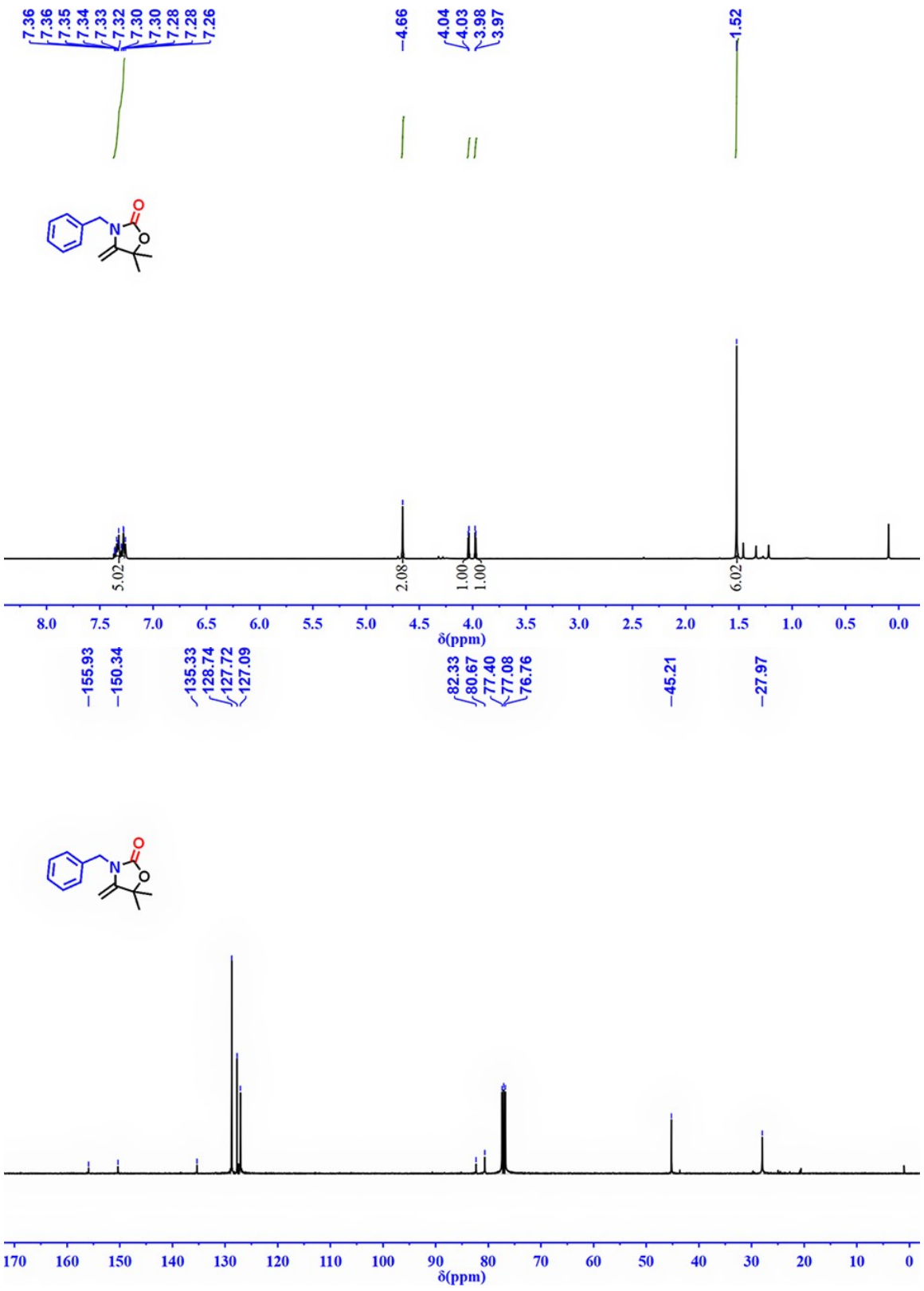

Fig. S16 ^{1}H and ^{13}C NMR of 3-benzyl-5,5-dimethyl-4-methyleneoxazolidin-2-one (**2f**). ^{1}H NMR (400 MHz, Chloroform-d): δ 7.37 – 7.27 (m, 5H), 4.67 – 4.65 (s, 2H), 4.05 – 4.03 (d, J=3.0, 1H), 3.98 – 3.96 (d, J=3.0, 1H), 1.53 – 1.50 (s, 6H). ^{13}C NMR (101 MHz, $CDCl_3$): δ 155.93, 150.34, 135.33, 128.74, 127.72, 127.09, 82.33, 80.67, 45.21, 27.97.

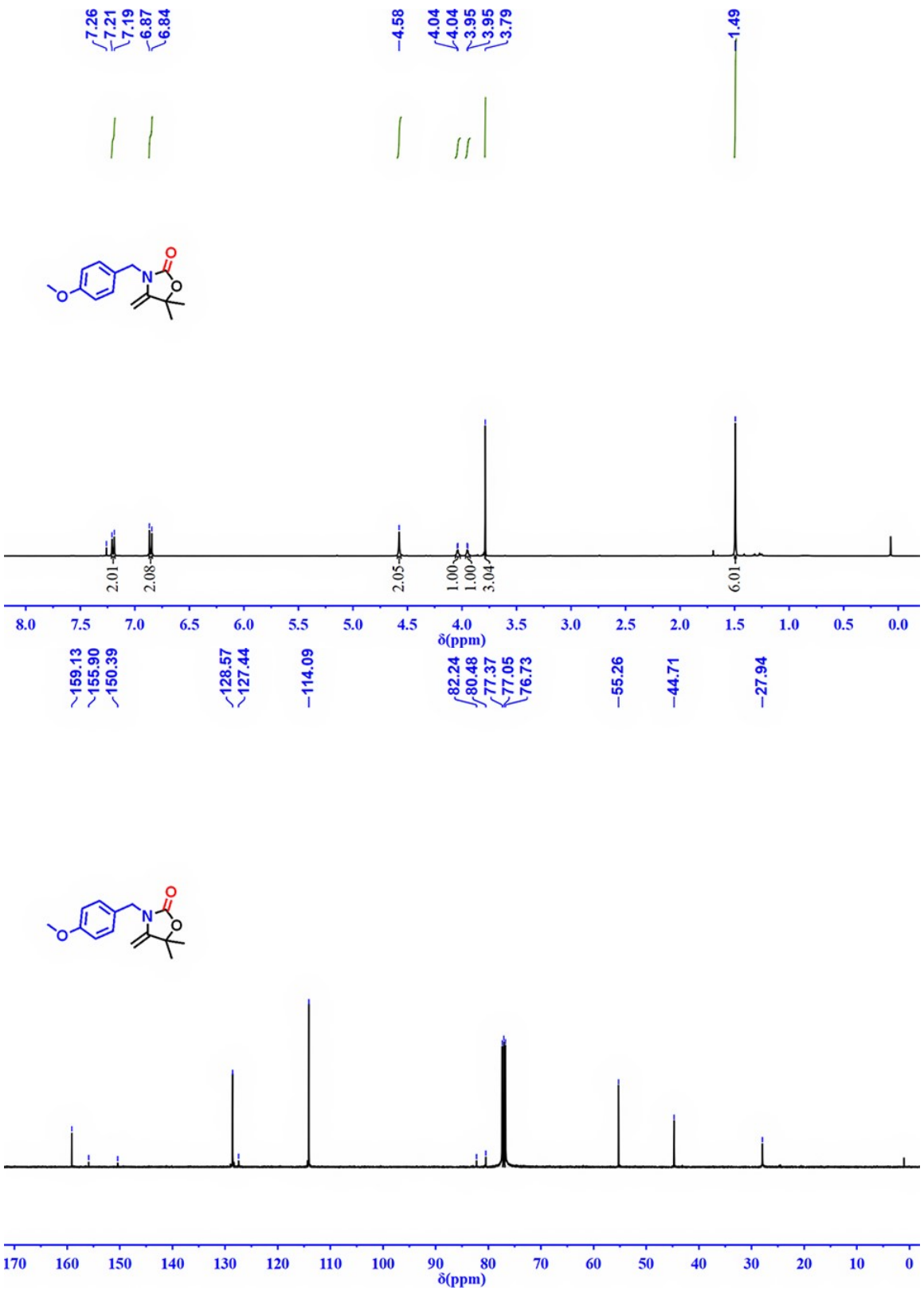

Fig. S17 ^{1}H and ^{13}C NMR of 3-(4-methoxybenzyl)-5,5-dimethyl-4-methyleneoxazolidin-2-one (**2g**). ^{1}H NMR (400 MHz, Chloroform-d): δ = 7.21 – 7.18 (d, J=8.7, 2H), 6.87 – 6.84 (d, J=8.7, 2H), 4.59 – 4.56 (s, 2H), 4.06 – 4.02 (d, J=2.5, 1H), 3.97 – 3.93 (d, J=2.5, 1H), 3.79 – 3.78 (s, 3H), 1.50 – 1.49 (s, 6H). ^{13}C NMR (101 MHz, $CDCl_3$): δ 159.13, 155.90, 150.39, 128.57, 127.44, 114.09, 82.24, 80.48, 55.26, 44.71, 27.94.

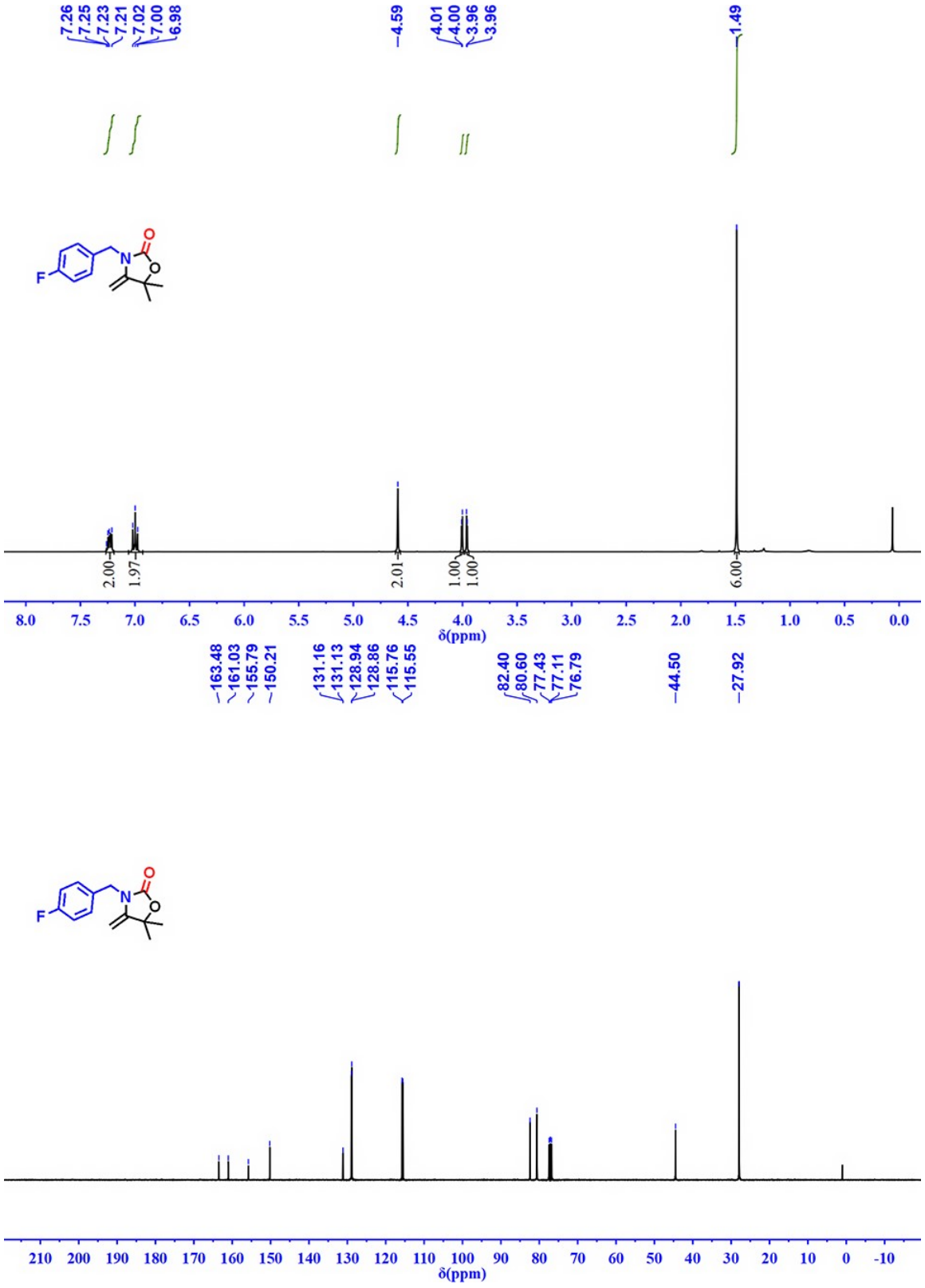

Fig. S18 ^{1}H and ^{13}C NMR of 3-(4-fluorobenzyl)-5,5-dimethyl-4-methyleneoxazolidin-2-one (**2h**). ^{1}H NMR (400 MHz, Chloroform-d): δ 7.27 – 7.19 (m, 2H), 7.05 – 6.95 (t, J=8.7, 2H), 4.61 – 4.57 (s, 2H), 4.02 – 3.99 (d, J=3.1, 1H), 3.98 – 3.94 (d, J=3.1, 1H), 1.53 – 1.44 (s, 6H). ^{13}C NMR (101 MHz, $CDCl_3$): δ 163.48, 161.03, 155.79, 150.21, 131.16 – 131.13 (d, J=3.3), 128.94 – 128.86 (d, J=8.2), 115.76 – 115.55 (d, J=21.7), 82.40, 80.60, 44.50, 27.92.

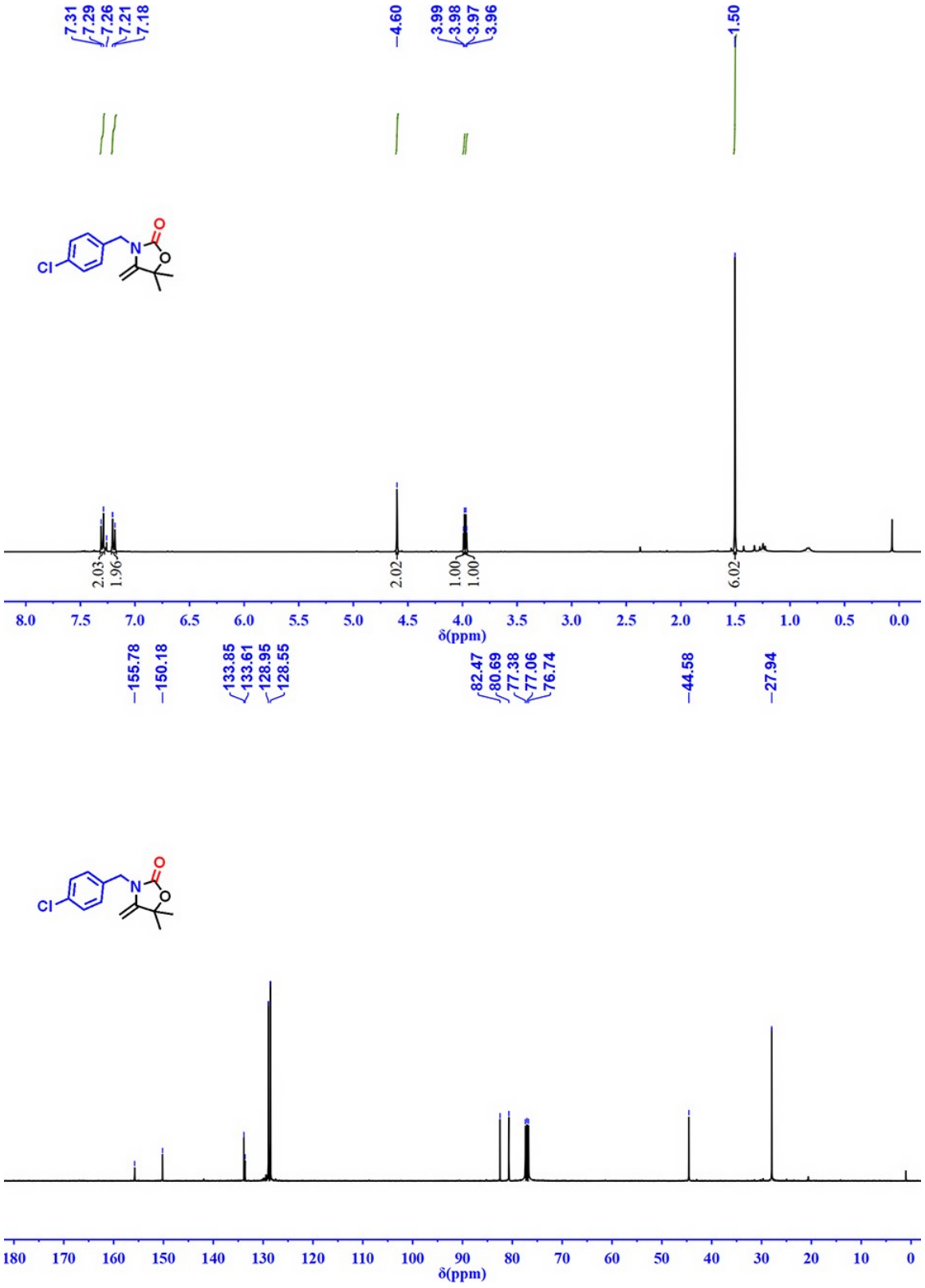

Fig. S19 ^{1}H and ^{13}C NMR of 3-(4-chlorobenzyl)-5,5-dimethyl-4-methyleneoxazolidin-2-one (**2i**). ^{1}H NMR (400 MHz, Chloroform-d): δ 7.32 – 7.28 (d, J=8.5, 2H), 7.21 – 7.17 (d, J=8.7, 2H), 4.61 – 4.59 (s, 2H), 4.00 – 3.98 (d, J=3.1, 1H), 3.97 – 3.95 (d, J=3.1, 1H), 1.51 – 1.49 (s, 6H). ^{13}C NMR (101 MHz, $CDCl_3$): δ 155.78, 150.18, 133.85, 133.61, 128.95, 128.55, 82.47, 80.69, 44.58, 27.94.

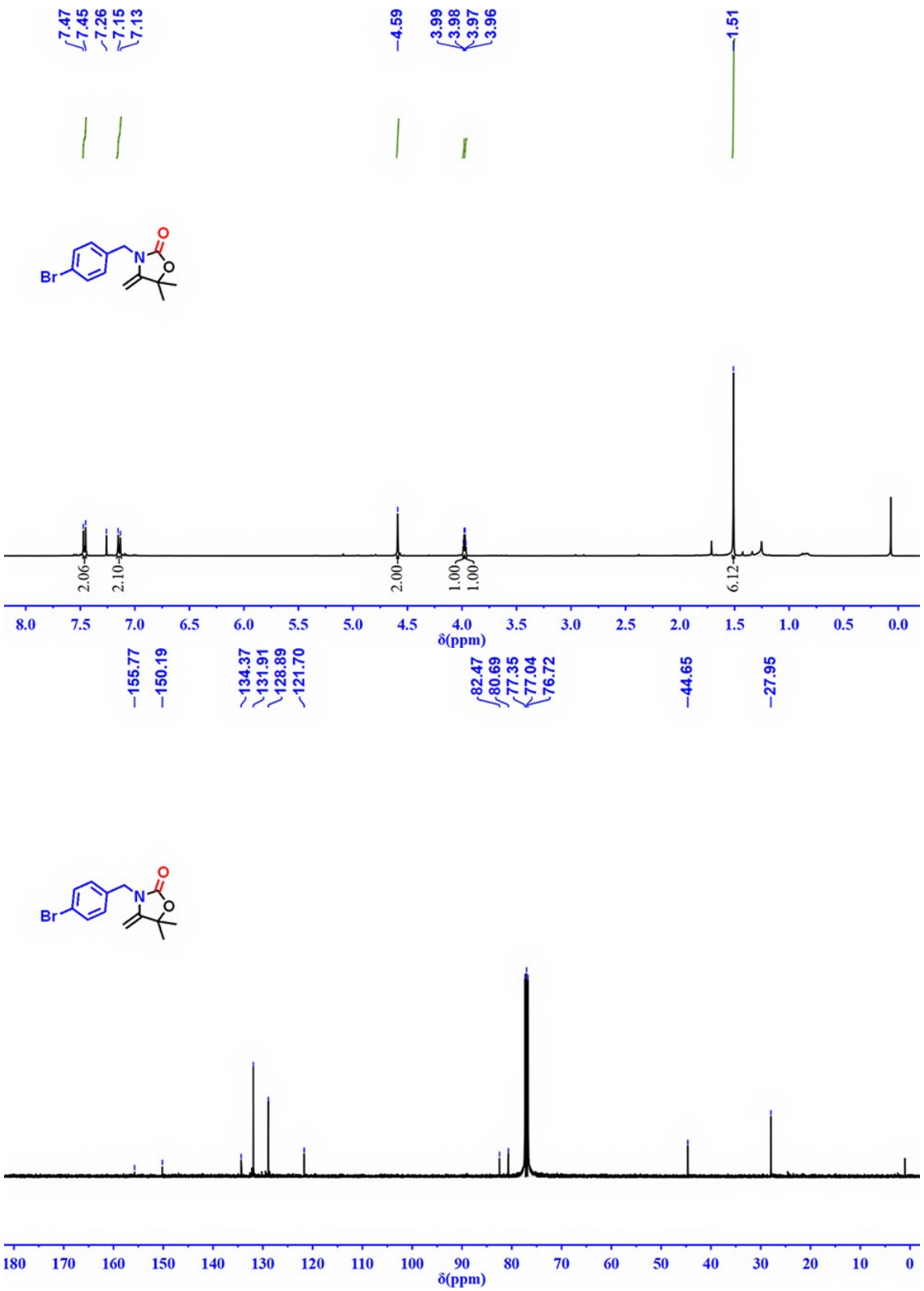

Fig. S20 ^{1}H and ^{13}C NMR of 3-(4-bromobenzyl)-5,5-dimethyl-4-methyleneoxazolidin-2-one (**2j**). ^{1}H NMR (400 MHz, Chloroform-d): δ 7.48 – 7.45 (d, J=8.4, 2H), 7.16 – 7.12 (d, J=8.4, 2H), 4.60 – 4.58 (s, 2H), 3.99 – 3.98 (d, J=3.1, 1H), 3.98 – 3.96 (d, J=3.1, 1H), 1.52 – 1.50 (s, 6H). ^{13}C NMR (101 MHz, $CDCl_3$): δ 155.77, 150.19, 134.37, 131.91, 128.89, 121.70, 82.47, 80.69, 44.65, 27.95.

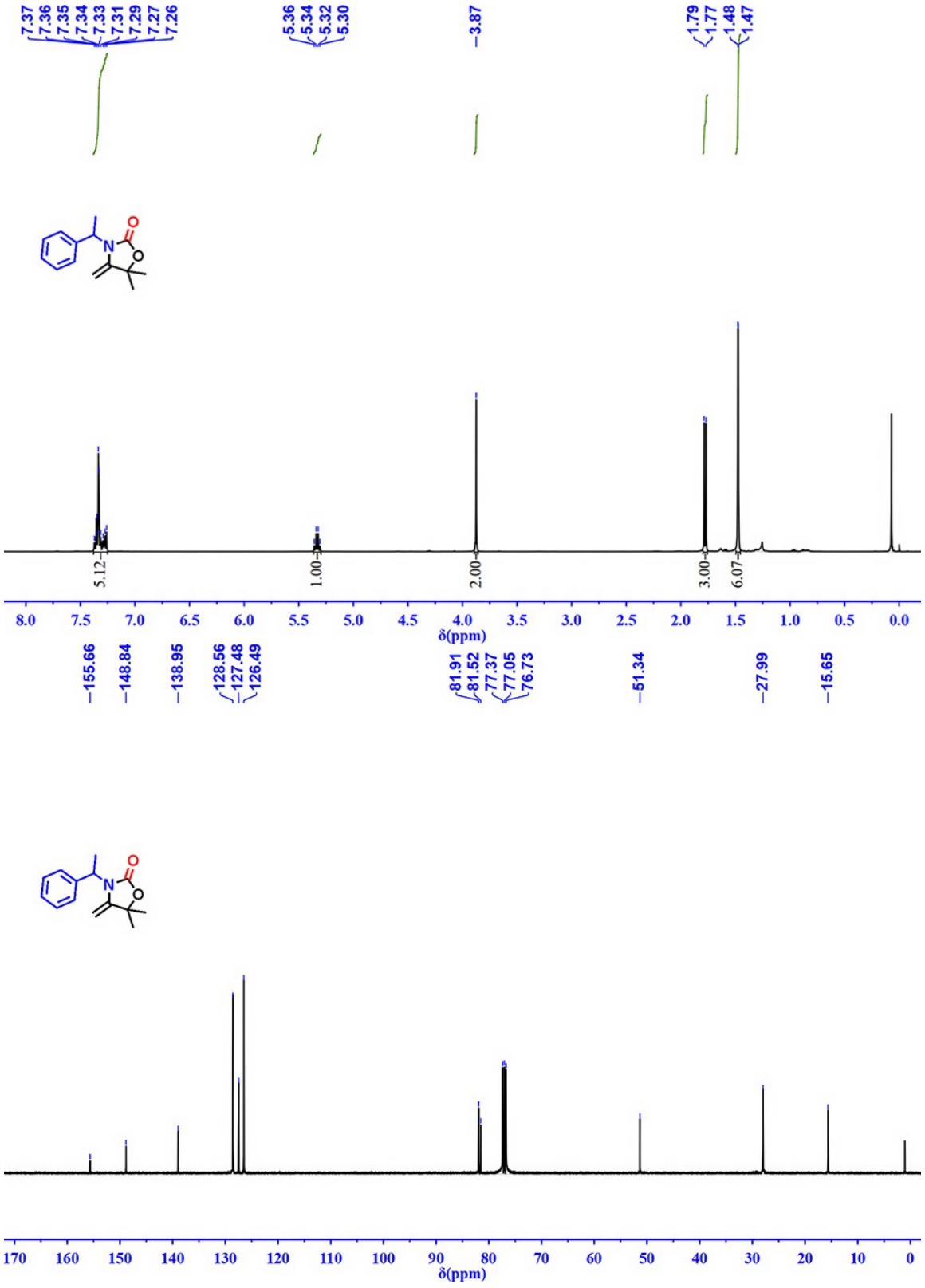

Fig. S21 ^{1}H and ^{13}C NMR of 5,5-dimethyl-4-methylene-3-(1-phenylethyl)oxazolidin-2-one (**2k**). ^{1}H NMR (400 MHz, Chloroform-d): δ 7.38 – 7.25 (m, 5H), 5.36 – 5.30 (q, J=7.2, 1H), 3.89 – 3.86 (s, 2H), 1.80 – 1.76 (d, J=7.2, 3H), 1.49 – 1.46 (d, J=1.6, 6H). ^{13}C NMR (101 MHz, $CDCl_3$): δ 155.66, 148.84, 138.95, 128.56, 127.48, 126.49, 81.91, 81.52, 51.34, 27.99, 15.65.

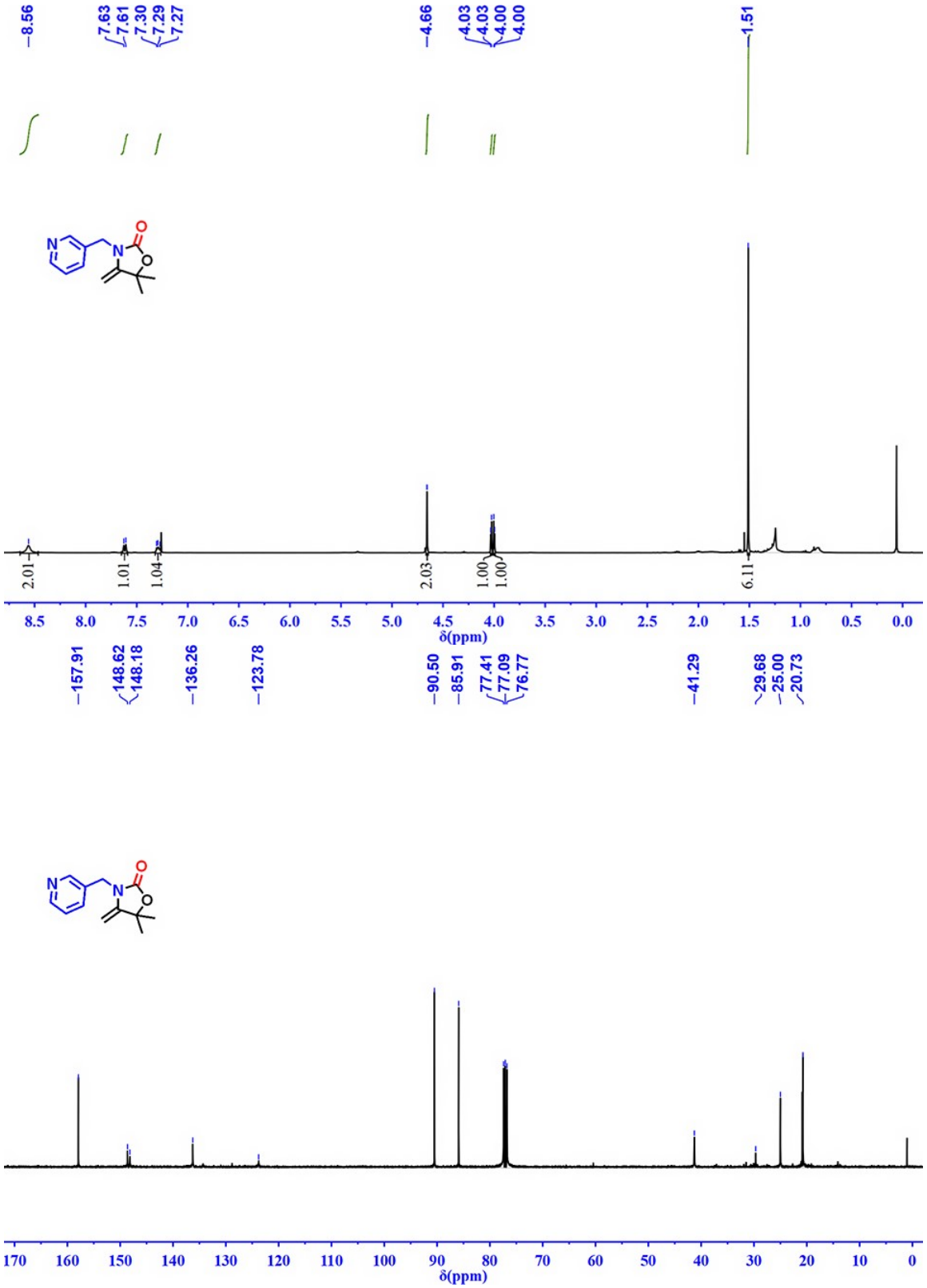

Fig. S22 ^{1}H and ^{13}C NMR of 5,5-dimethyl-4-methylene-3-(pyridin-3-ylmethyl)oxazolidin-2-one (**2l**). ^{1}H NMR (400 MHz, Chloroform-d): δ = 8.64 – 8.47 (s, 2H), 7.65 – 7.59 (d, J=7.9, 1H), 7.32 – 7.26 (m, 1H), 4.67 – 4.64 (s, 2H), 4.04 – 4.02 (d, J=3.3, 1H), 4.01 – 3.99 (d, J=3.3, 1H), 1.52 – 1.50 (s, 6H). ^{13}C NMR (101 MHz, $CDCl_3$): δ 157.91, 148.62, 148.18, 136.26, 123.78, 90.50, 85.91, 41.29, 29.68, 25.00, 20.73.

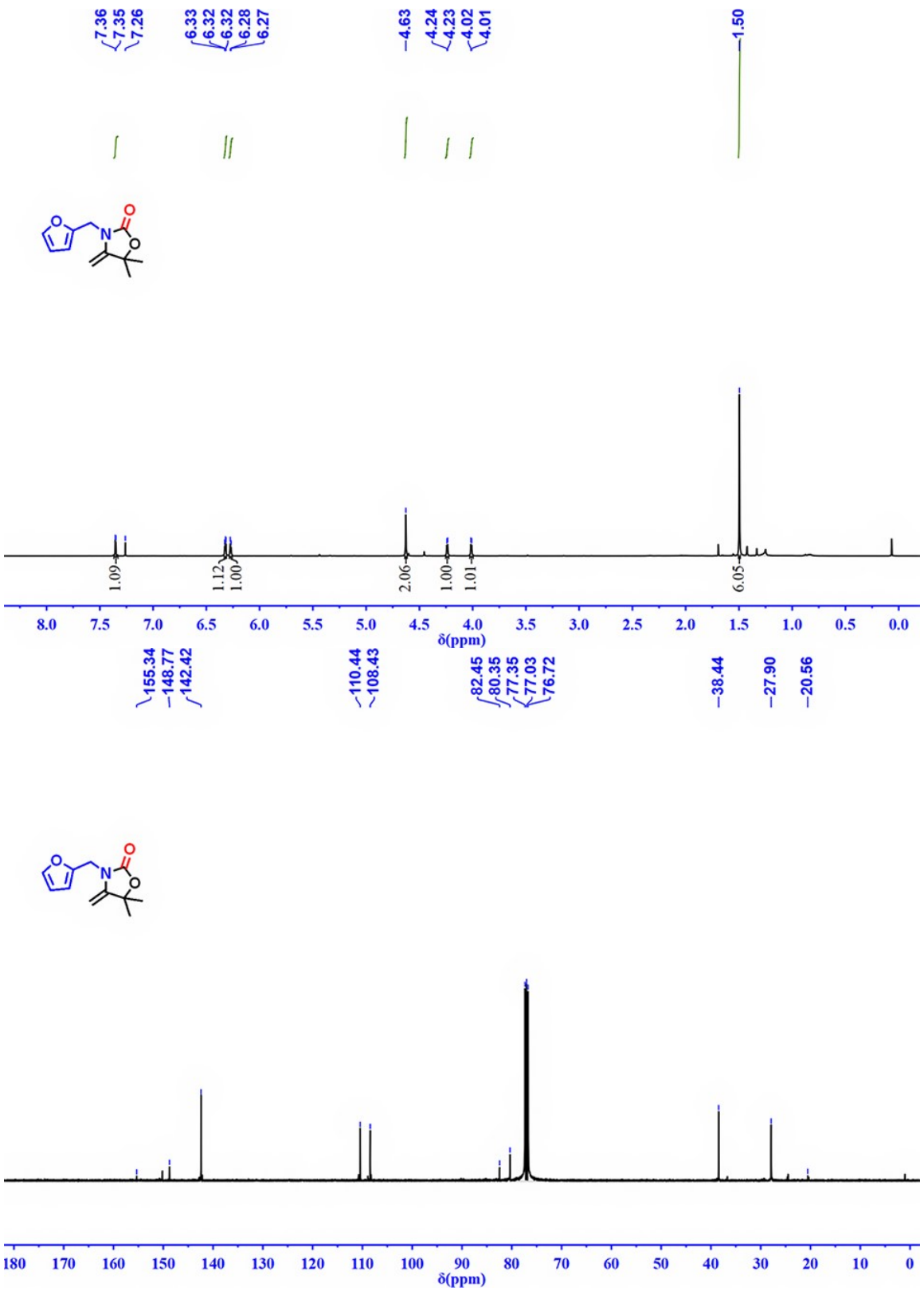

Fig. S23 ^{1}H and ^{13}C NMR of 3-(furan-2-ylmethyl)-5,5-dimethyl-4-methyleneoxazolidin-2-one (**2m**). ^{1}H NMR (400 MHz, Chloroform-d): δ 7.37 – 7.33 (d, J=2.5, 1H), 6.33 – 6.31 (m, 1H), 6.29 – 6.26 (d, J=3.2, 1H), 4.64 – 4.61 (s, 2H), 4.25 – 4.22 (d, J=3.0, 1H), 4.03 – 3.99 (d, J=3.0, 1H), 1.50 – 1.49 (s, 6H). ^{13}C NMR (101 MHz, $CDCl_3$): δ 155.34, 148.77, 142.42, 110.44, 108.43, 82.45, 80.35, 38.44, 27.90, 20.56.

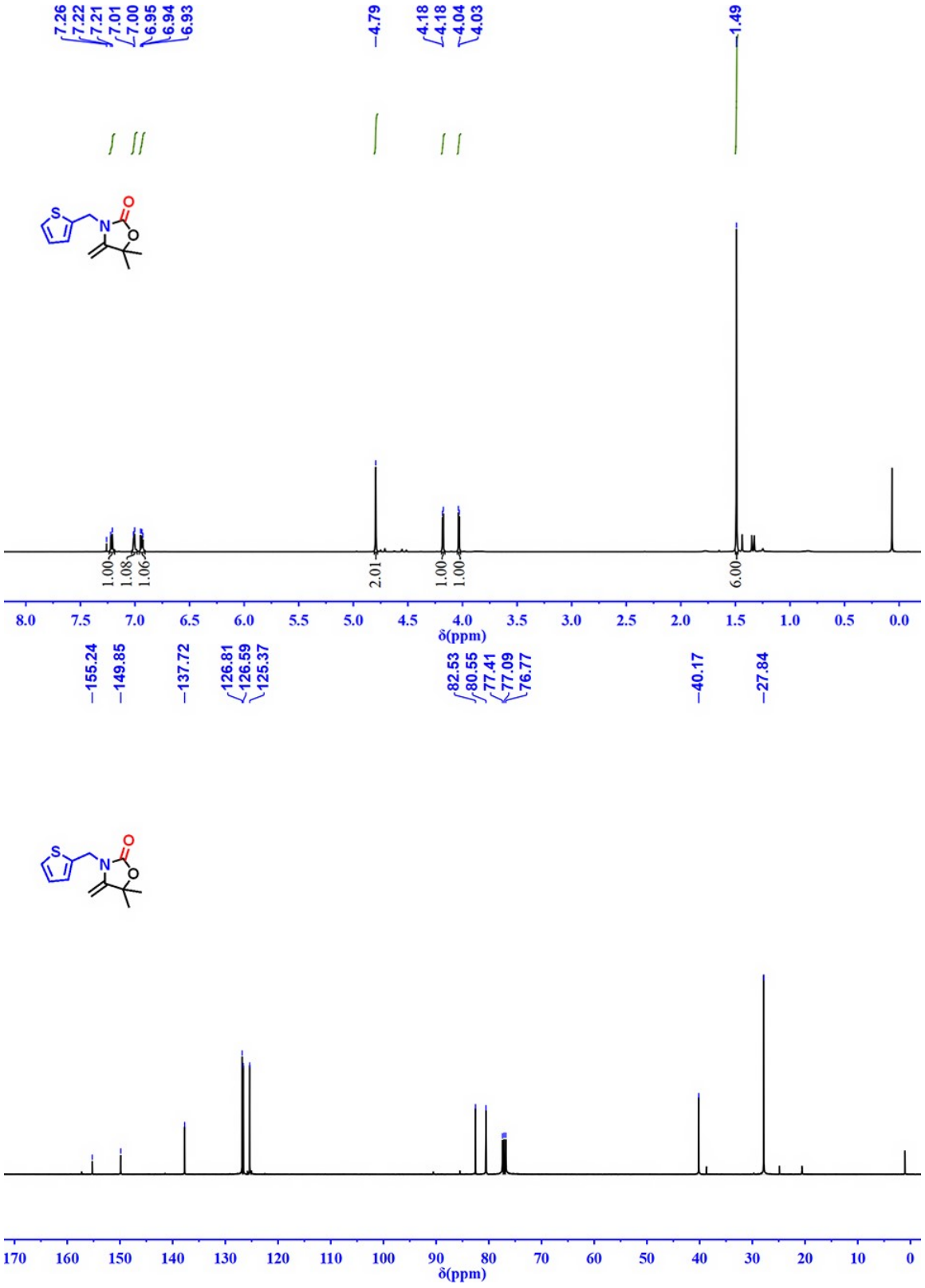

Fig. S24 ^{1}H and ^{13}C NMR of 5,5-dimethyl-4-methylene-3-(thiophen-2-ylmethyl)oxazolidin-2-one (**2n**). ^{1}H NMR (400 MHz, Chloroform-d): δ 7.24 – 7.19 (d, J=6.3, 1H), 7.03 – 6.98 (d, J=4.3, 1H), 6.96 – 6.91 (m, 1H), 4.81 – 4.78 (s, 2H), 4.19 – 4.16 (d, J=3.2, 1H), 4.05 – 4.02 (d, J=3.2, 1H), 1.50 – 1.48 (s, 6H). ^{13}C NMR (101 MHz, $CDCl_3$): δ 155.24, 149.85, 137.72, 126.81, 126.59, 125.37, 82.53, 80.55, 40.17, 27.84.

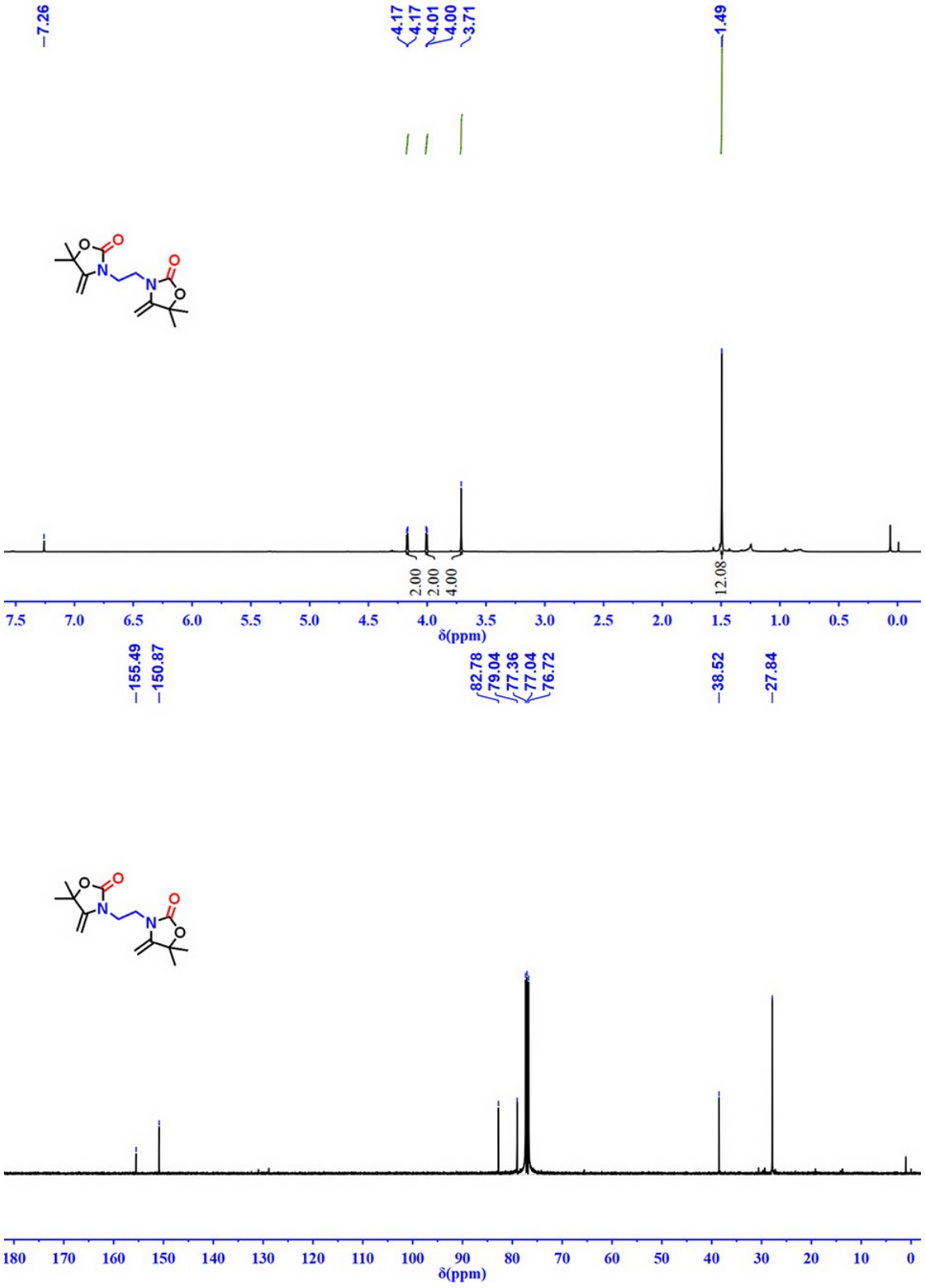

Fig. S25 ^{1}H and ^{13}C NMR of 3,3'-(ethane-1,2-diyl)bis(5,5-dimethyl-4-methyleneoxazolidin-2-one) (**2o**). ^{1}H NMR (400 MHz, Chloroform-d): δ 4.18 – 4.16 (d, J=3.3, 2H), 4.01 – 4.00 (d, J=3.3, 2H), 3.72 – 3.70 (s, 4H), 1.50 – 1.49 (s, 12H). ^{13}C NMR (101 MHz, $CDCl_3$): δ 155.49, 150.87, 82.78, 79.04, 38.52, 27.84.

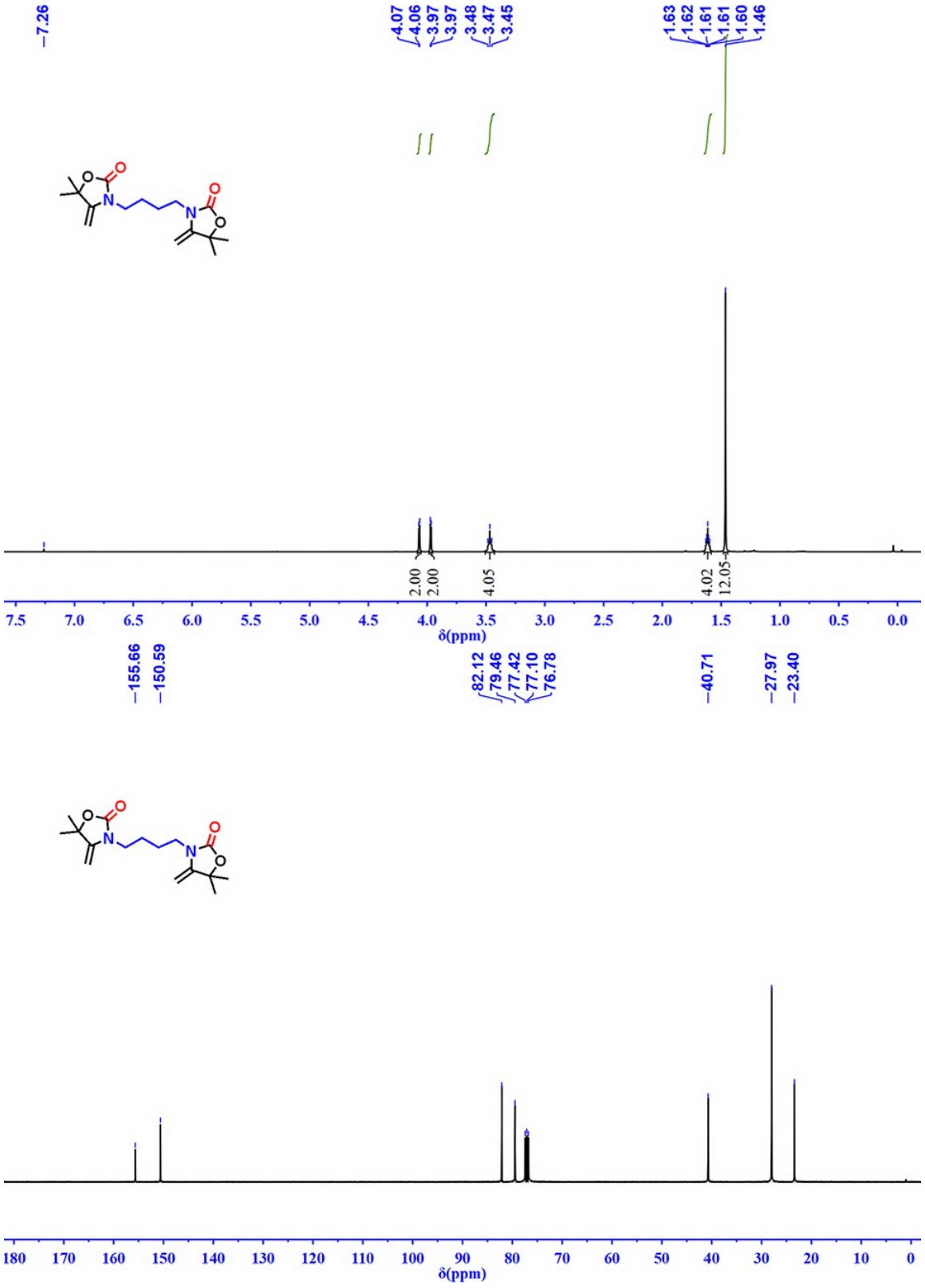

Fig. S26 ^{1}H and ^{13}C NMR of 3,3'-(butane-1,4-diyl)bis(5,5-dimethyl-4-methyleneoxazolidin-2-one) (**2p**). ^{1}H NMR (400 MHz, Chloroform-d): δ 4.08 – 4.05 (d, J=3.1, 2H), 3.98 – 3.96 (d, J=3.1, 2H), 3.51 – 3.43 (m, 4H), 1.64 – 1.58 (m, 4H), 1.48 – 1.44 (s, 12H). ^{13}C NMR (101 MHz, $CDCl_3$): δ 155.66, 150.59, 82.12, 79.46, 40.71, 27.97, 23.40.

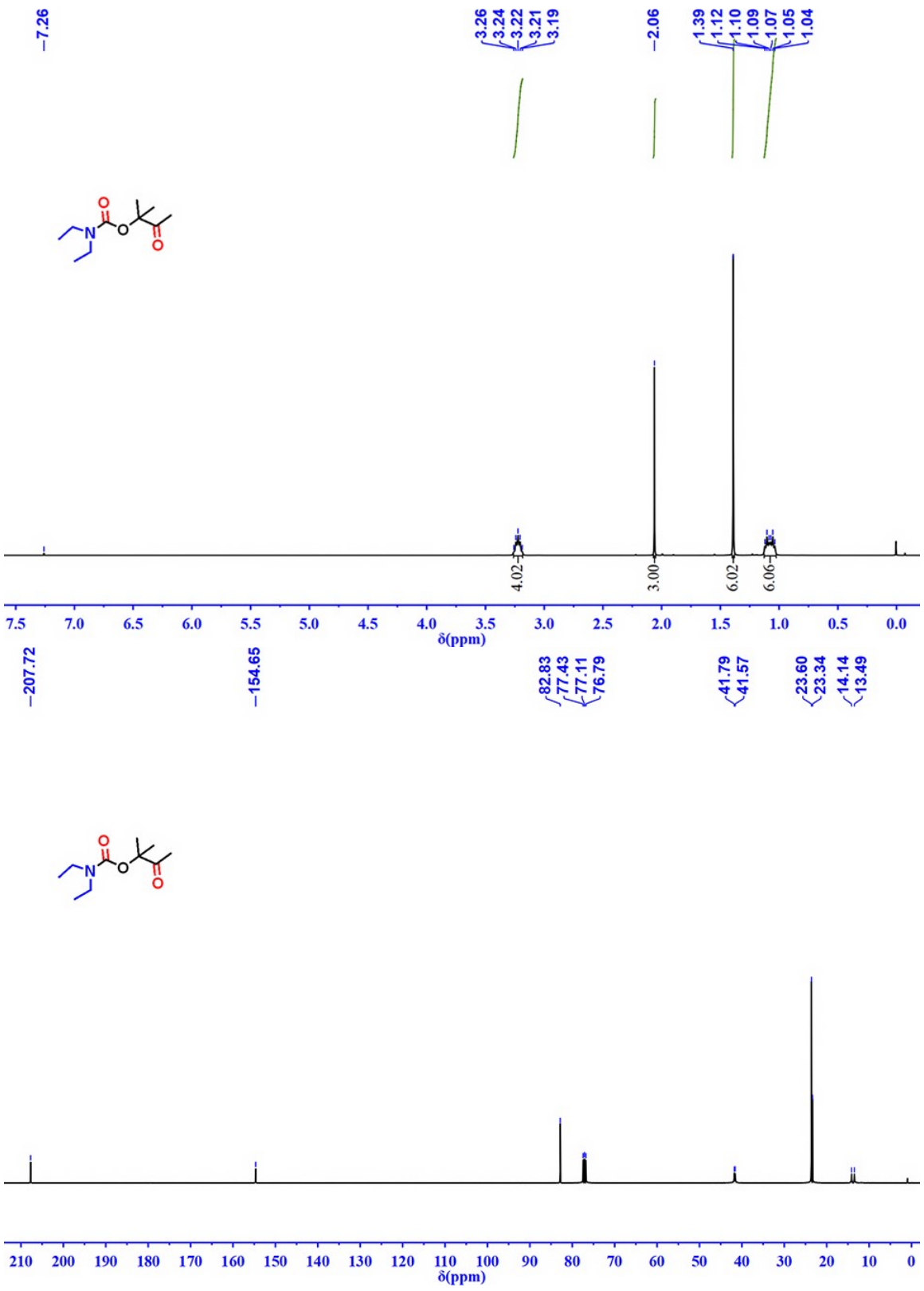

Fig. S27 ^{1}H and ^{13}C NMR of 2-methyl-3-oxobutan-2-yl diethylcarbamate (**2q**). ^{1}H NMR (400 MHz, Chloroform-d): δ 3.26 – 3.18 (p, J=7.1, 4H), 2.07 – 2.05 (s, 3H), 1.40 – 1.38 (s, 6H), 1.13 – 1.03 (dt, J=7.1, 19.9, 6H). ^{13}C NMR (101 MHz, $CDCl_3$): δ 207.72, 154.65, 82.83, 41.79, 41.57, 23.60, 23.34, 14.14, 13.49.

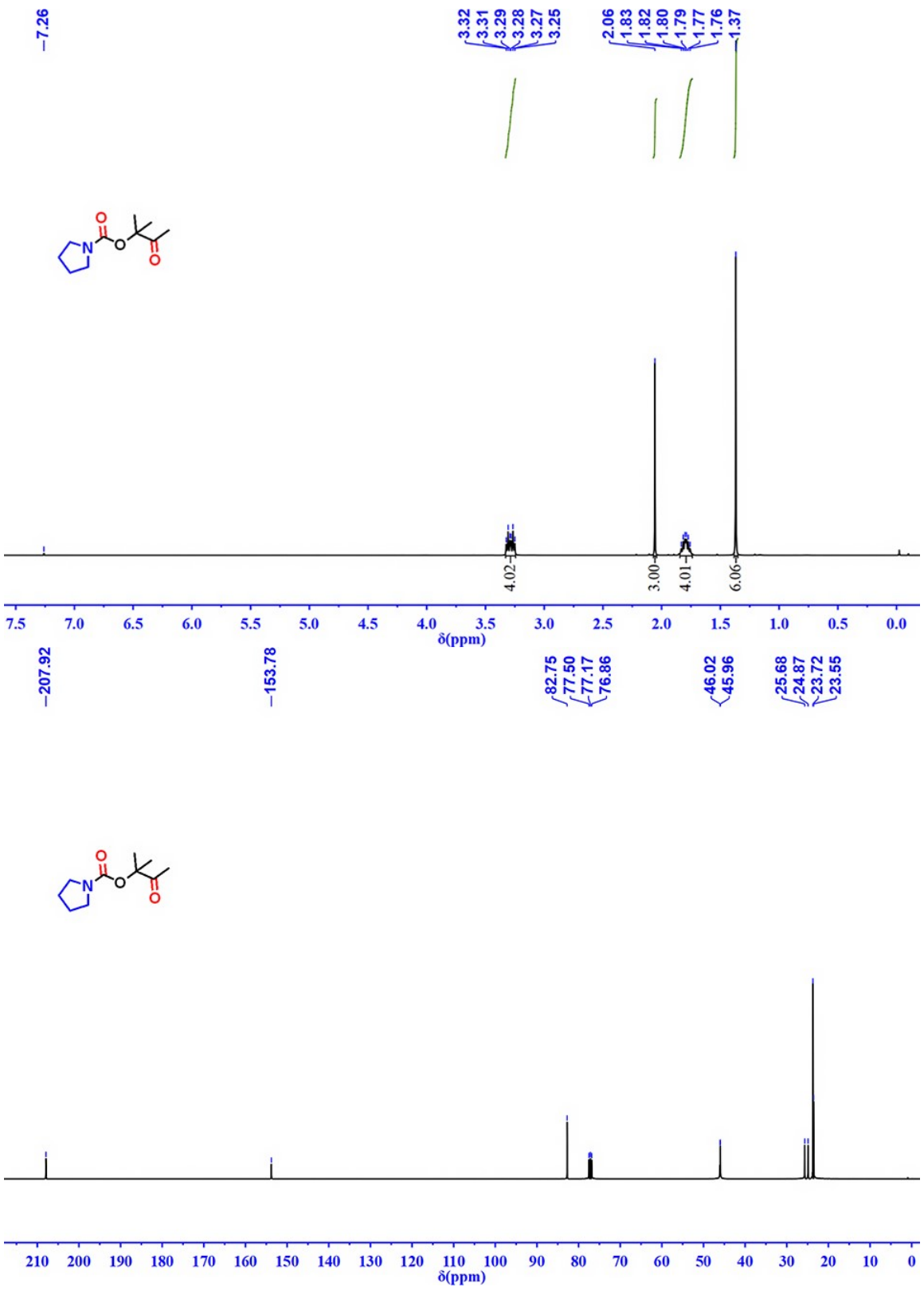

Fig. S28 ^{1}H and ^{13}C NMR of 2-methyl-3-oxobutan-2-yl pyrrolidine-1-carboxylate (**2r**). ^{1}H NMR (400 MHz, Chloroform-d): δ 3.33 – 3.24 (dt, J=6.6, 16.3, 4H), 2.07 – 2.04 (s, 3H), 1.84 – 1.74 (dq, J=6.7, 12.6, 4H), 1.38 – 1.35 (s, 6H). ^{13}C NMR (101 MHz, $CDCl_3$): δ 207.92, 153.78, 82.75, 46.02, 45.96, 25.68, 24.87, 23.72, 23.55.

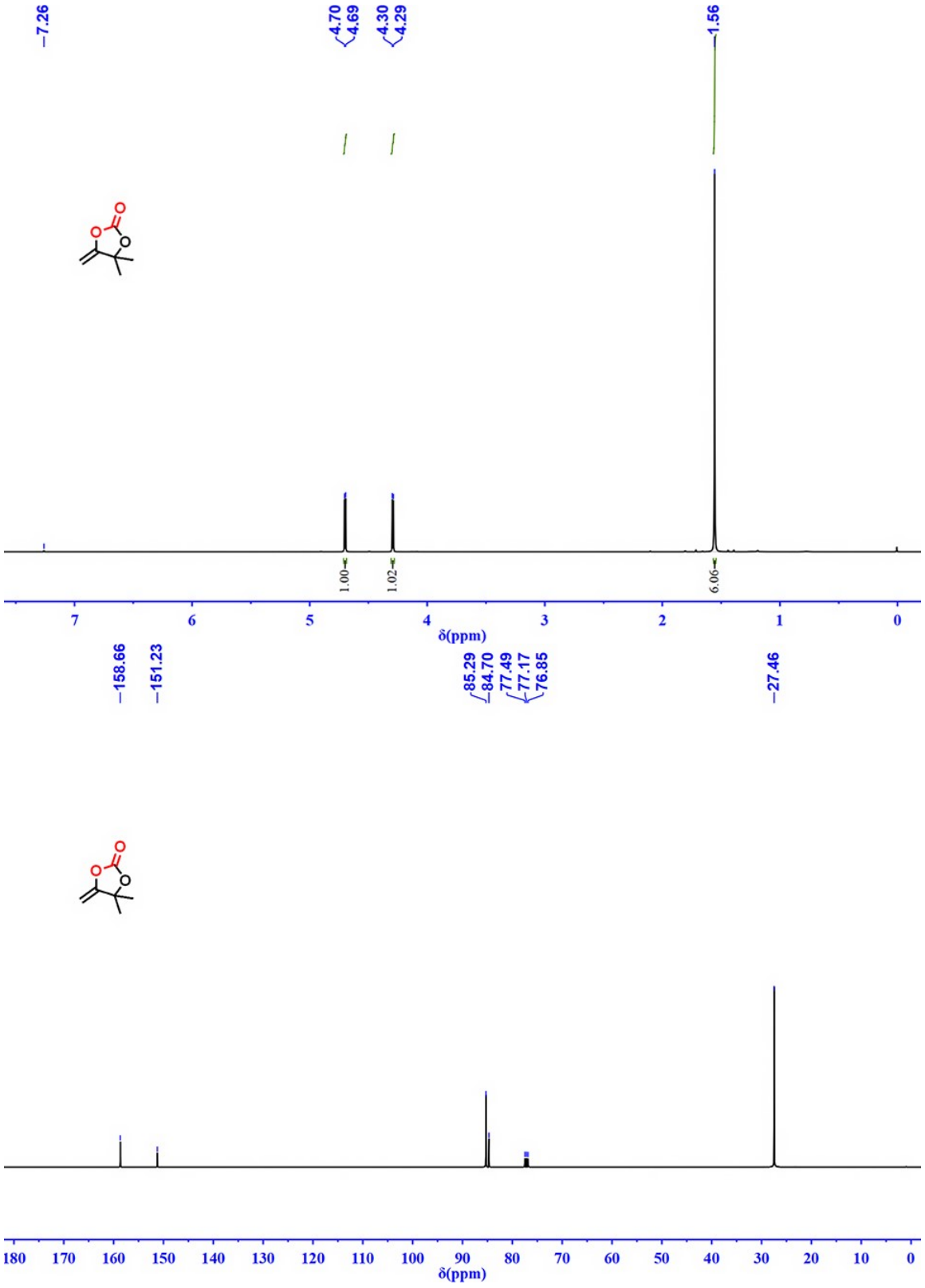

Fig. S29 ^{1}H and ^{13}C NMR of 4,4-dimethyl-5-methylene-1,3-dioxolan-2-one (**2s**). ^{1}H NMR (400 MHz, Chloroform-d): δ 4.71 – 4.69 (d, J=4.0, 1H), 4.31 – 4.28 (d, J=4.0, 1H), 1.57 – 1.54 (s, 6H). ^{13}C NMR (101 MHz, $CDCl_3$): δ 158.66, 151.23, 85.29, 84.70, 27.46.

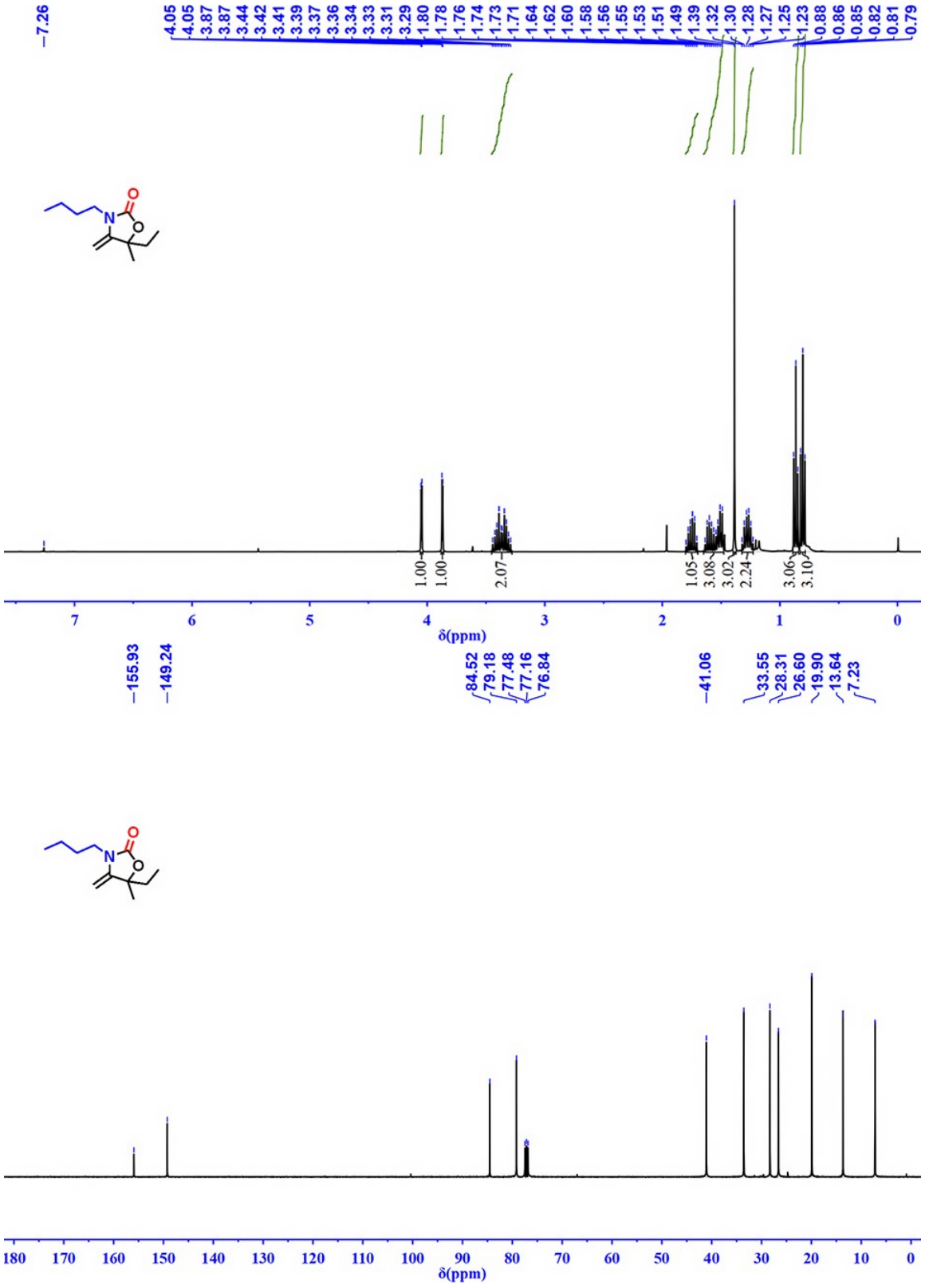

Fig. S30 ^{1}H and ^{13}C NMR of 3-butyl-5-ethyl-5-methyl-4-methyleneoxazolidin-2-one (**4a**). ^{1}H NMR (400 MHz, Chloroform-d): δ 4.06 – 4.04 (d, J=2.9, 1H), 3.88 – 3.86 (d, J=2.9, 1H), 3.45 – 3.28 (m, 2H), 1.80 – 1.70 (dq, J=7.3, 14.6, 1H), 1.65 – 1.48 (m, 3H), 1.40 – 1.37 (s, 3H), 1.32 – 1.23 (dq, J=7.4, 14.7, 2H), 0.89 – 0.84 (t, J=7.4, 3H), 0.83 – 0.78 (t, J=7.4, 3H). ^{13}C NMR (101 MHz, $CDCl_3$): δ 155.93, 149.24, 84.52, 79.18, 41.06, 33.55, 28.31, 26.60, 19.90, 13.64, 7.23.

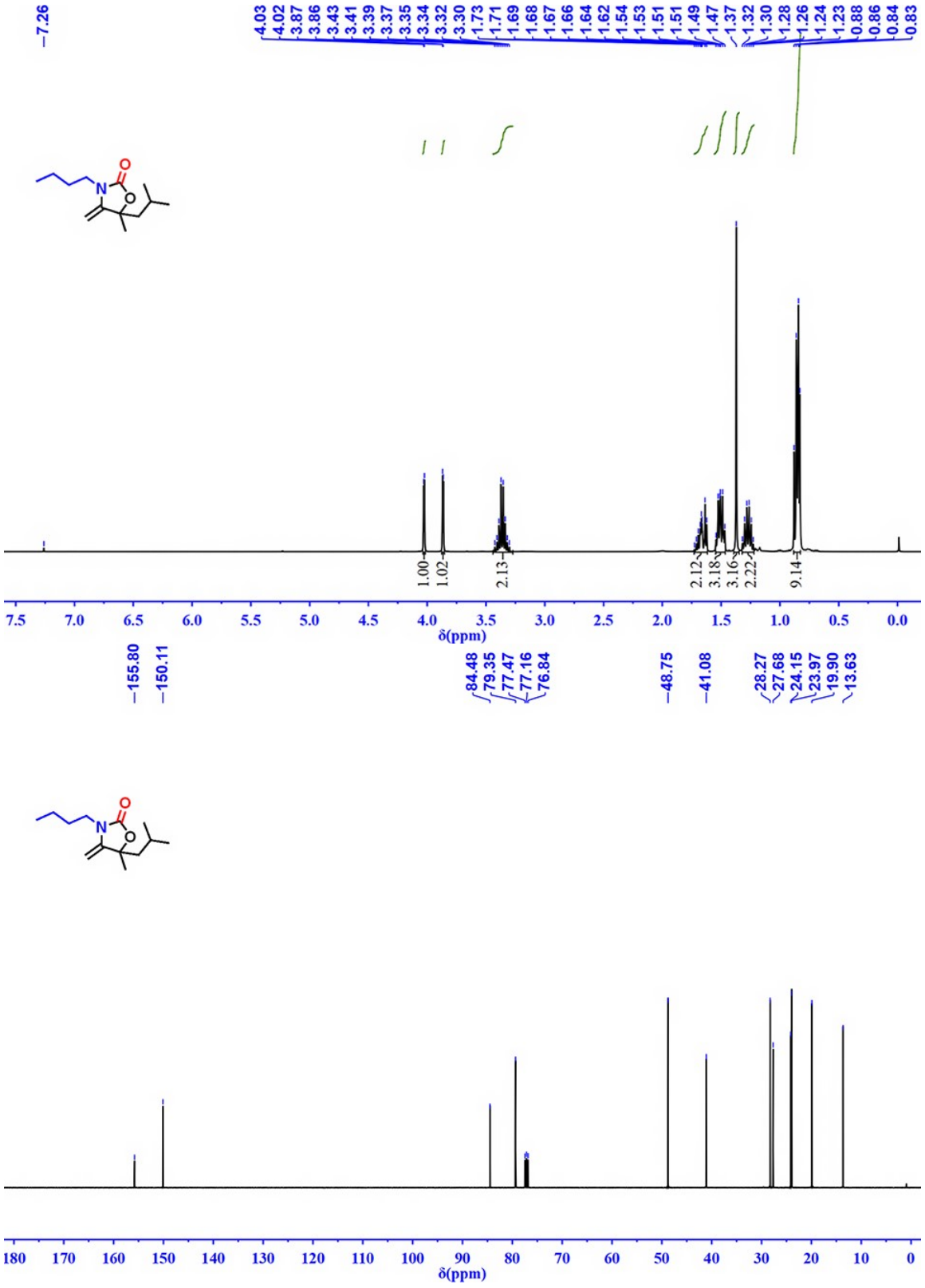

Fig. S31 ^{1}H and ^{13}C NMR of 3-butyl-5-isobutyl-5-methyl-4-methyleneoxazolidin-2-one (**4b**). ^{1}H NMR (400 MHz, Chloroform-d): δ 4.04 – 4.02 (d, J=2.9, 1H), 3.88 – 3.85 (d, J=2.9, 1H), 3.44 – 3.27 (hept, J=7.0, 2H), 1.73 – 1.62 (m, 2H), 1.56 – 1.46 (m, 3H), 1.39 – 1.35 (s, 3H), 1.32 – 1.22 (dq, J=7.4, 14.6, 2H), 0.88 – 0.83 (m, 9H). ^{13}C NMR (101 MHz, $CDCl_3$): δ 155.80, 150.11, 84.48, 79.35, 48.75, 41.08, 28.27, 27.68, 24.15, 23.97, 19.90, 13.63.

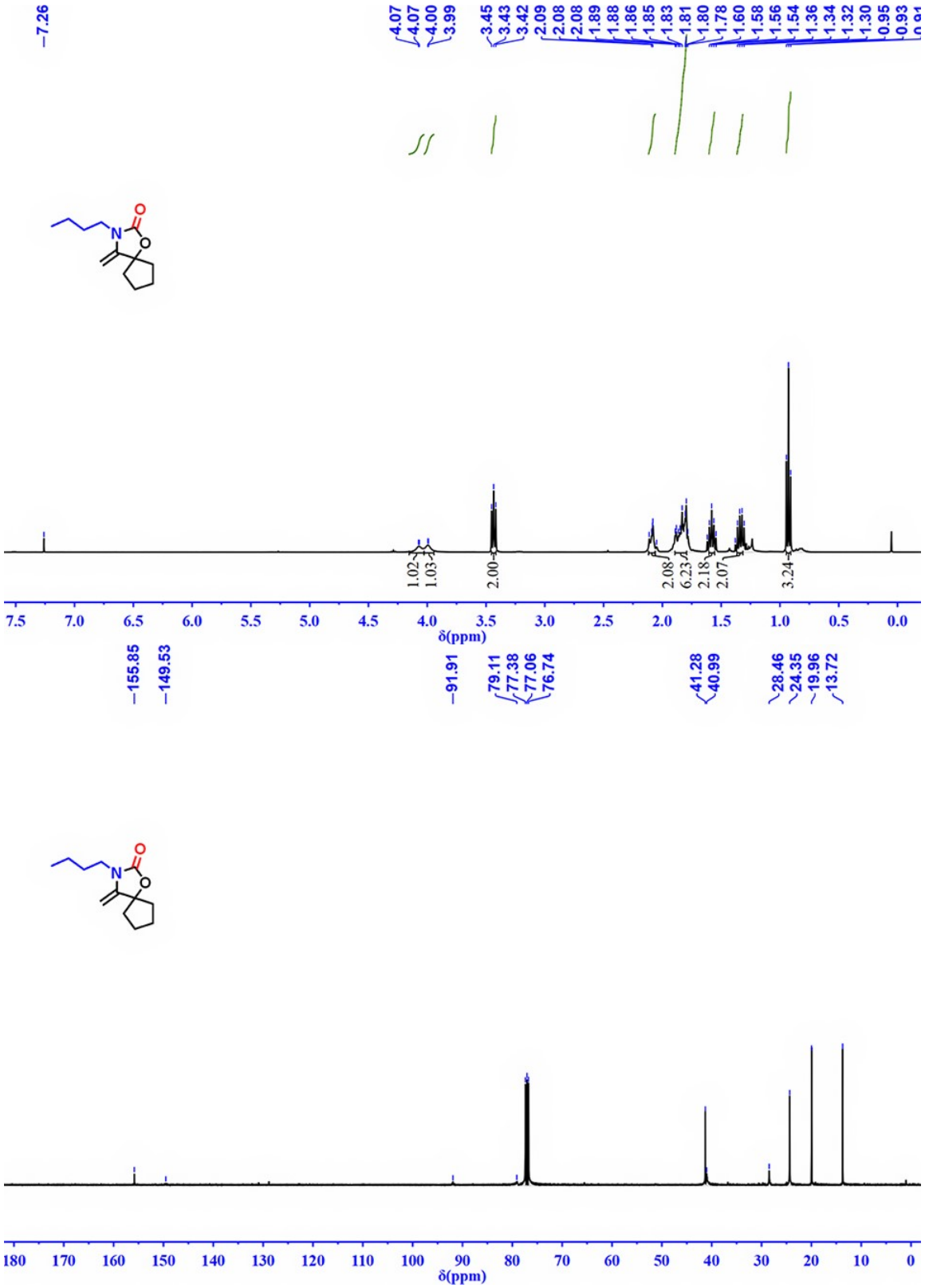

Fig. S32 ^{1}H and ^{13}C NMR of 3-butyl-4-methylene-1-oxa-3-azaspiro[4.4]nonan-2-one (**4c**). ^{1}H NMR (400 MHz, Chloroform-d): δ 4.15 – 4.03 (m, 1H), 4.03 – 3.94 (m, 1H), 3.45 – 3.42 (m, 2H), 2.12 – 2.06 (m, 2H), 1.89 – 1.79 (m, 6H), 1.60 – 1.56 (t, J=7.5, 2H), 1.37 – 1.32 (m, 2H), 0.95 – 0.91 (t, J=7.3, 3H). ^{13}C NMR (101 MHz, $CDCl_3$): δ 155.85, 149.53, 91.91, 79.11, 41.28, 41.99, 28.46, 24.35, 19.96, 13.72.

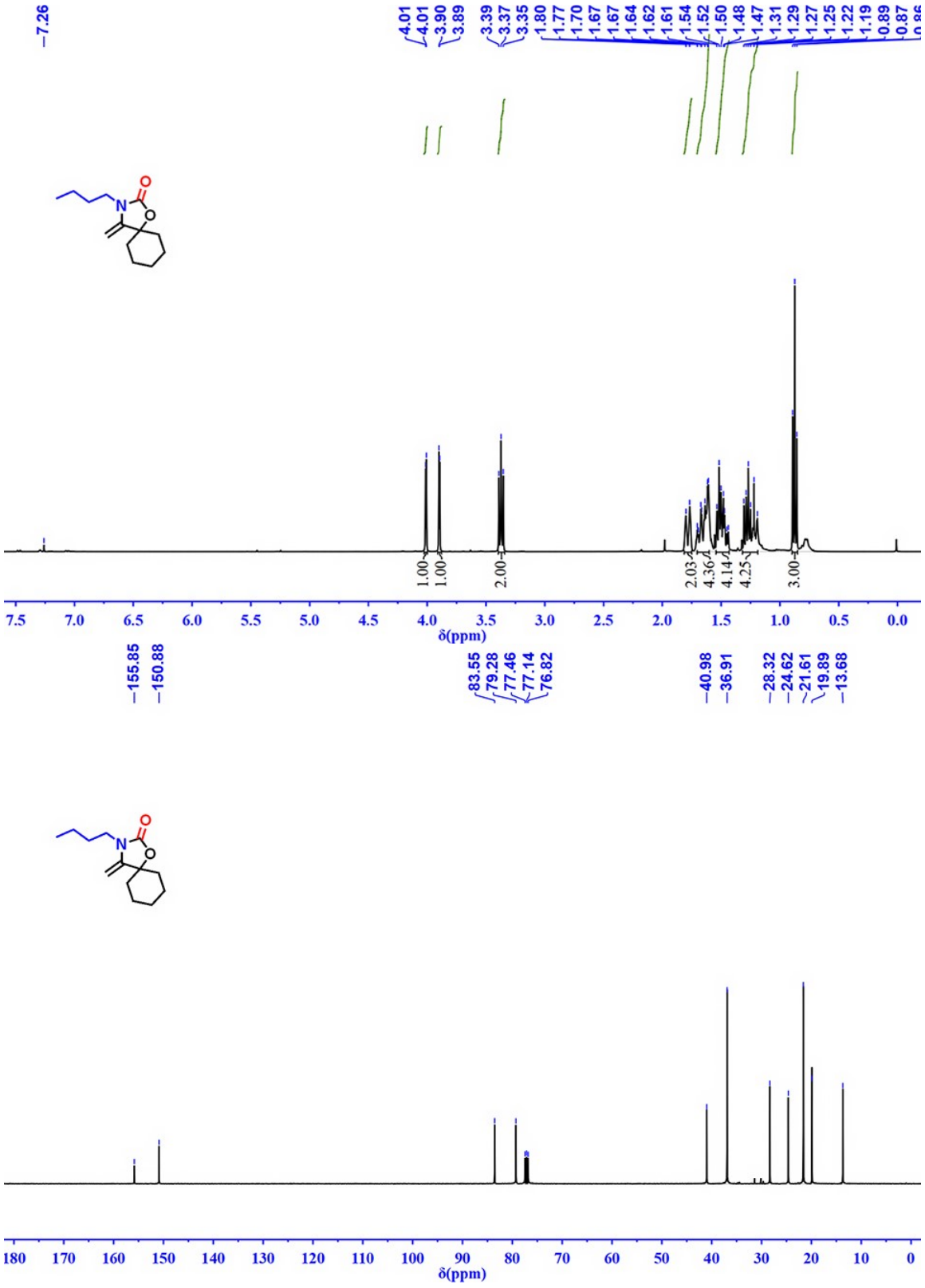

Fig. S33 ^{1}H and ^{13}C NMR of 3-butyl-4-methylene-1-oxa-3-azaspiro[4.5]decan-2-one (**4d**). ^{1}H NMR (400 MHz, Chloroform-d): δ 4.03 – 4.00 (d, J=2.8, 1H), 3.91 – 3.88 (d, J=2.8, 1H), 3.40 – 3.34 (m, 2H), 1.81 – 1.75 (d, J=12.4, 2H), 1.70 – 1.60 (m, 4H), 1.54 – 1.43 (m, 4H), 1.32 – 1.19 (m, 4H), 0.90 – 0.85 (t, J=7.4, 3H). ^{13}C NMR (101 MHz, $CDCl_3$): δ 155.85, 150.88, 83.55, 79.28, 40.98, 36.91, 28.32, 24.62, 21.61, 19.89, 13.68.

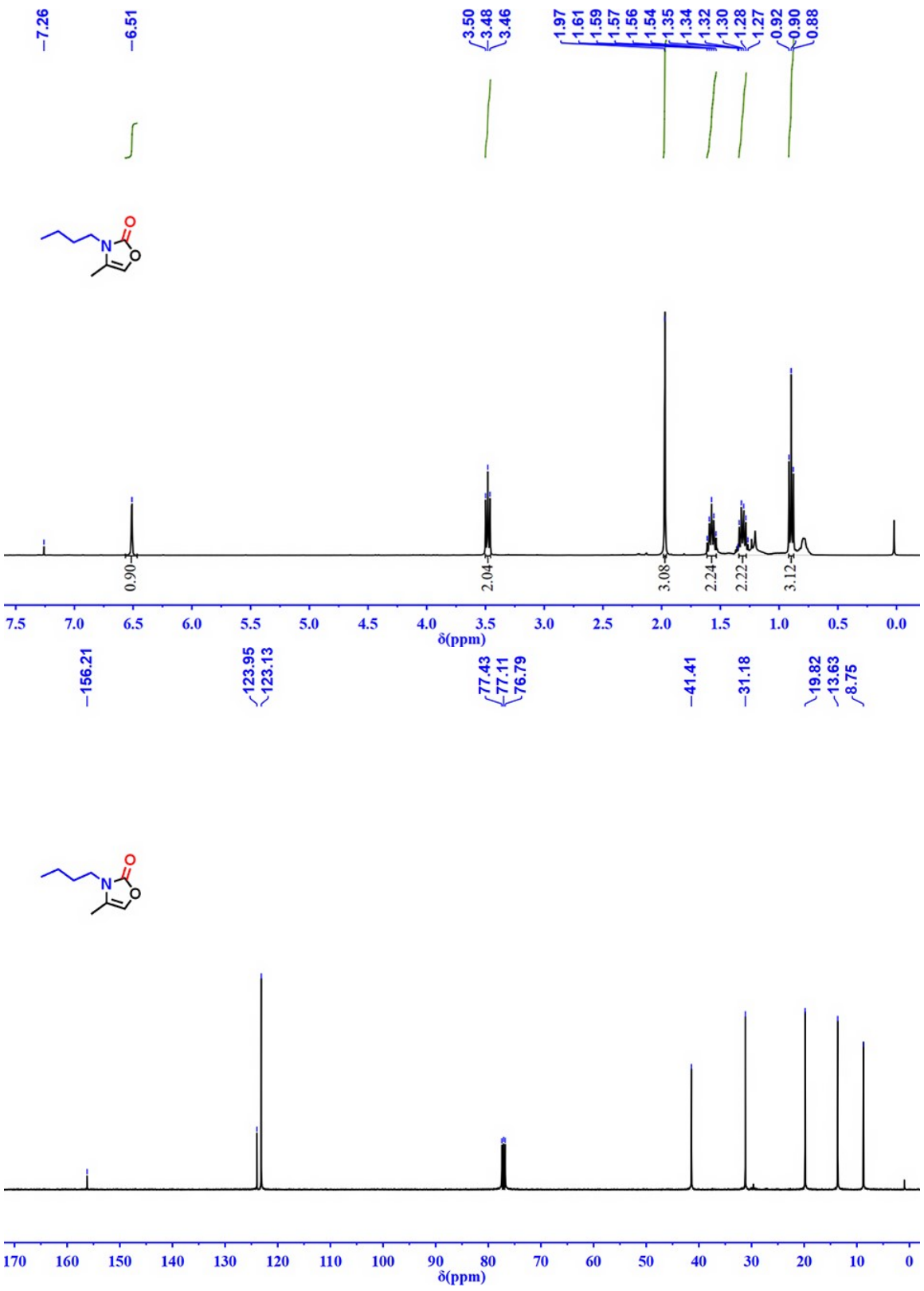

Fig. S34 ^{1}H and ^{13}C NMR of 3-butyl-4-methyloxazol-2(3H)-one (**4e**). ^{1}H NMR (400 MHz, Chloroform-d): δ 6.57 – 6.47 (s, 1H), 3.50 – 3.46 (m, 2H), 1.98 – 1.96 (s, 3H), 1.61 – 1.54 (p, J=7.6, 2H), 1.34 – 1.28 (m, 2H), 0.92 – 0.88 (t, J=7.3, 3H). ^{13}C NMR (101 MHz, $CDCl_3$): δ 156.21, 123.95, 123.13, 41.41, 31.18, 19.82, 13.63, 8.75.

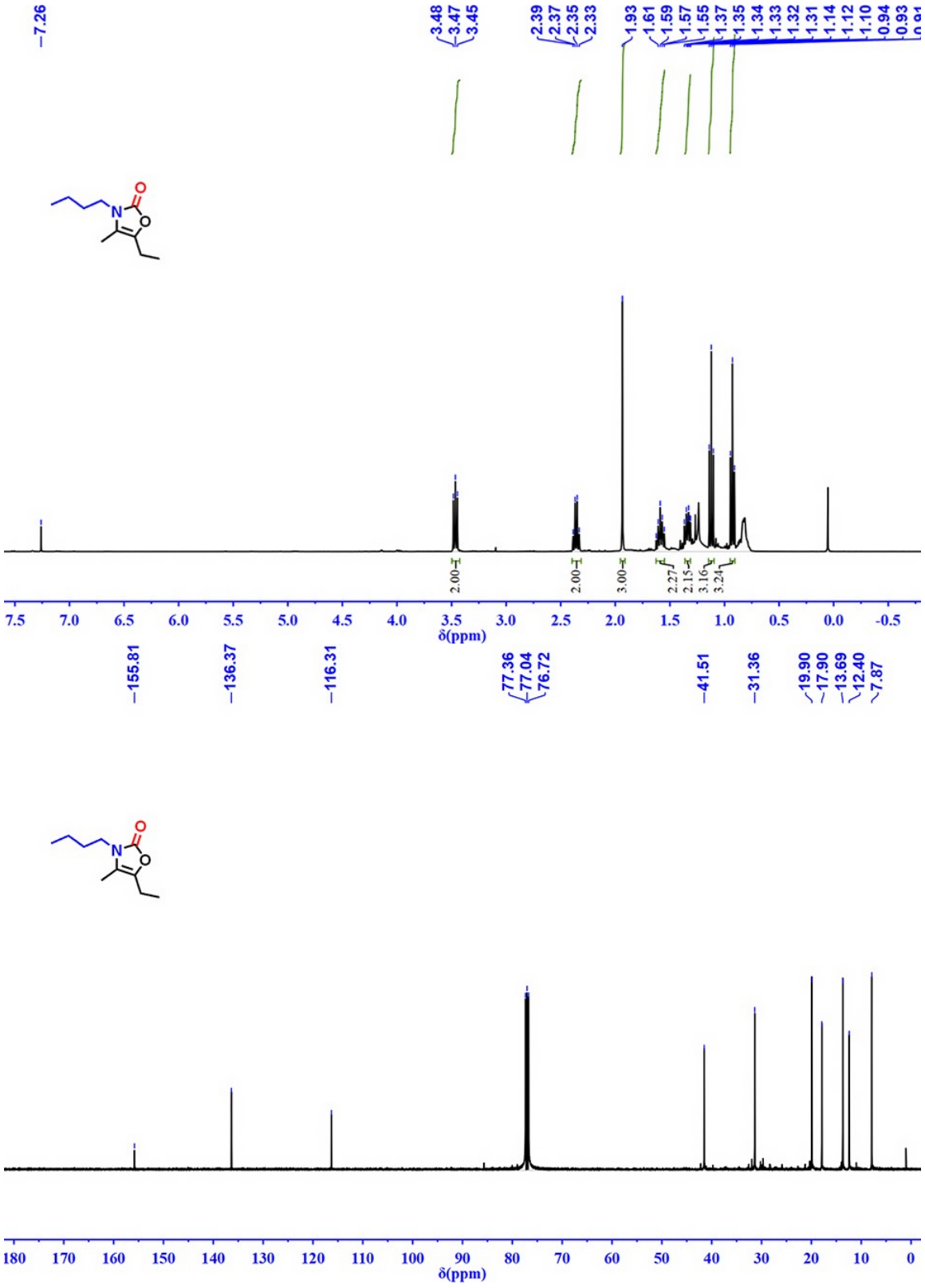

Fig. S35 ^{1}H and ^{13}C NMR of 3-butyl-5-ethyl-4-methyloxazol-2(3H)-one (**4f**). ^{1}H NMR (400 MHz, Chloroform-d): δ 3.50 – 3.43 (m, 2H), 2.40 – 2.31 (q, J=7.5, 2H), 1.95 – 1.91 (s, 3H), 1.63 – 1.55 (p, J=7.5, 2H), 1.36 – 1.31 (dd, J=5.2, 7.9, 2H), 1.15 – 1.10 (t, J=7.5, 3H), 0.95 – 0.91 (t, J=7.3, 3H). ^{13}C NMR (101 MHz, $CDCl_3$): δ 155.81, 136.37, 116.31, 41.51, 31.36, 19.90, 17.90, 13.69, 12.40, 7.87.

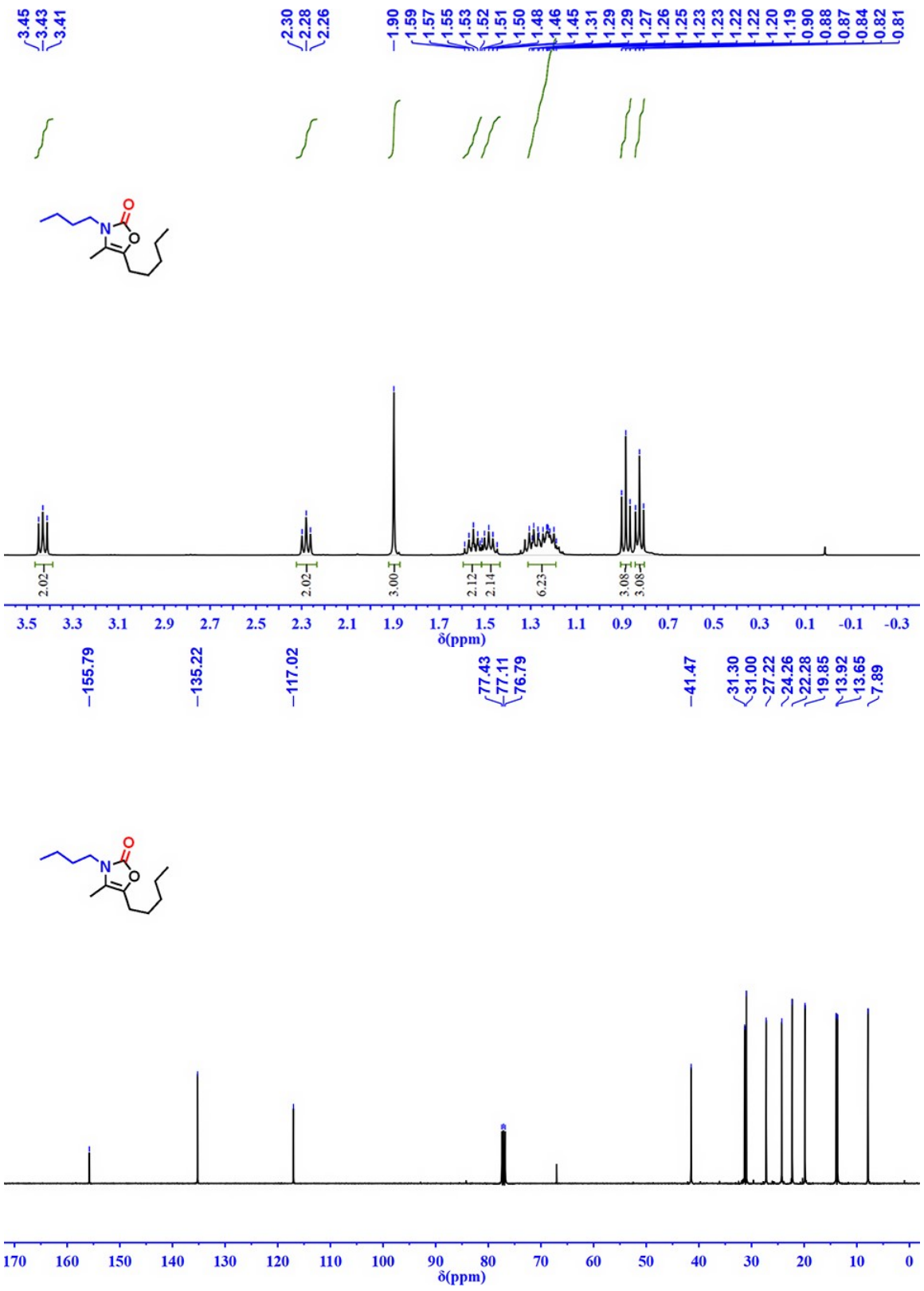

Fig. S36 ^{1}H and ^{13}C NMR of 3-butyl-4-methyl-5-pentyloxazol-2(3H)-one (**4g**). ^{1}H NMR (400 MHz, Chloroform-d): δ 3.46 – 3.39 (m, 2H), 2.32 – 2.23 (t, J=7.3, 2H), 1.92 – 1.87 (s, 3H), 1.59 – 1.52 (m, 2H), 1.51 – 1.43 (m, 2H), 1.31 – 1.19 (m, 6H), 0.91 – 0.86 (t, J=7.3, 3H), 0.84 – 0.80 (t, J=7.0, 3H). ^{13}C NMR (101 MHz, $CDCl_3$): δ 155.79, 135.22, 117.02, 41.47, 31.30, 31.00, 27.22, 24.26, 22.28, 19.85, 13.92, 13.65, 7.89.

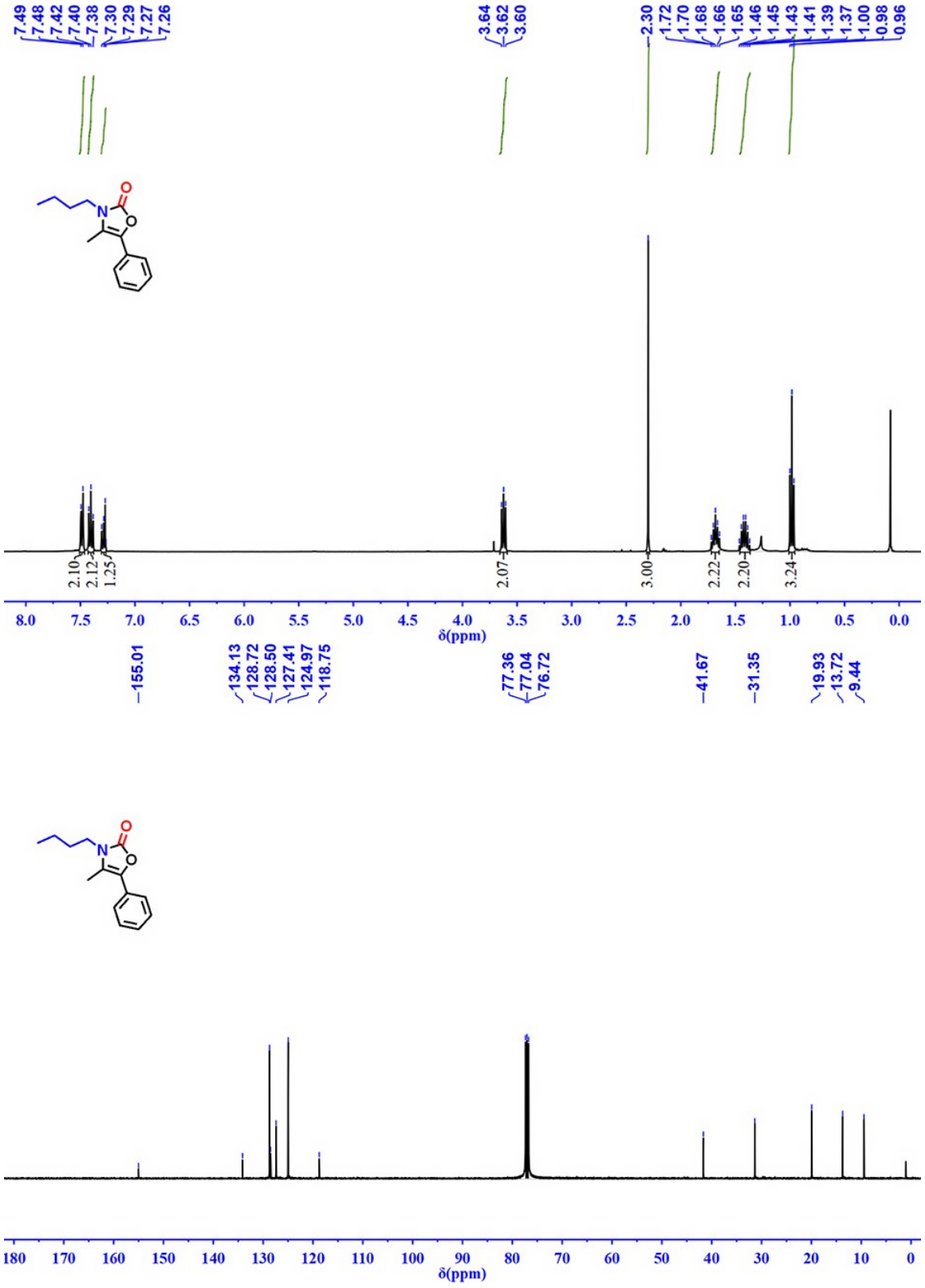

Fig. S37 ^{1}H and ^{13}C NMR of 3-butyl-4-methyl-5-phenyloxazol-2(3H)-one (**4h**). ^{1}H NMR (400 MHz, Chloroform-d): δ 7.51 – 7.46 (d, J=7.2, 2H), 7.43 – 7.38 (t, J=7.8, 2H), 7.31 – 7.27 (m, 1H), 3.66 – 3.59 (m, 2H), 2.31 – 2.29 (s, 3H), 1.72 – 1.65 (t, J=7.6, 2H), 1.46 – 1.37 (dt, J=7.4, 14.8, 2H), 1.01 – 0.96 (t, J=7.4, 3H). ^{13}C NMR (101 MHz, $CDCl_3$): δ 155.01, 134.13, 128.72, 128.50, 127.41, 124.97, 118.75, 41.67, 31.35, 19.93, 13.72, 9.44.

References

1. W.-C. Huang, L.-M. Lyu, Y.-C. Yang and M. H. Huang, *J. Am. Chem. Soc.*, 2012, **134**, 1261-1267.
2. Y. Wang, Y. Wang, L. Zhang, C.-S. Liu, H. Pang and Y. Wang, *Inorg. Chem. Front.*, 2019, **6**, 2514-2520.
3. C.-H. Zhang, T.-D. Hu, Y.-T. Zhai, Y.-X. Zhang and Z.-L. Wu, *Green Chem.*, 2023, **25**, 1938-1947.
4. J. Datka, E. Kukulska-Zając and W. Kobyzewa, *Catal. Today*, 2005, **101**, 123-129.
5. J. Zhou, S. Yang, W. Wan, L. Chen and J. Chen, *J. Catal.*, 2023, **418**, 178-189.
6. R. Das and C. M. Nagaraja, *Inorg. Chem.*, 2020, **59**, 9765-9773.
7. Z. Zhang, H. Gao, H. Wu, Y. Qian, L. Chen and J. Chen, *ACS Appl. Nano Mater.*, 2018, **1**, 6463-6476.
8. G. Zhang, H. Yang and H. Fei, *ACS Catal.*, 2018, **8**, 2519-2525.
9. D. K. Nandi, N. Haque, S. Biswas, N. A. Siddiqui, A. Khan, S. M. Islam and D. K. Nandi, *New J. Chem.*, 2024, **48**, 11982-11992.
10. Q.-W. Song, B. Yu, X.-D. Li, R. Ma, Z.-F. Diao, R.-G. Li, W. Li, L.-N. He and Q.-W. Song, *Green Chem.*, 2014, **16**, 1633-1638.
11. H.-F. Jiang and J.-W. Zhao, *Tetrahedron Lett.*, 2009, **50**, 60-62.
12. J. Xu, J. Zhao, Z. Jia and J. Zhang, *Synth. Commun.*, 2011, **41**, 858-863.
13. H. Jiang, J. Zhao and A. Wang, *Synthesis*, 2008, **2008**, 763-769.
14. J. Qiu, Y. Zhao, Y. Zhao, H. Wang, Z. Li, J. Wang and T. Jiao, *Molecules*, 2019, **24**, 1241.
15. Q. Zhang, F. Shi, Y. Gu, J. Yang and Y. Deng, *Tetrahedron Lett.*, 2005, **46**, 5907-5911.
16. Y. Gu, Q. Zhang, Z. Duan, J. Zhang, S. Zhang and Y. Deng, *J. Org. Chem.*, 2005, **70**, 7376-7380.
17. N. D. Ca, B. Gabriele, G. Ruffolo, L. Veltri, T. Zanetta and M. Costa, *Adv. Synth. Catal.*, 2011, **353**, 133-146.
18. H. Liu and R. Hua, *Tetrahedron*, 2016, **72**, 1200-1204.